

Testing Effective Yukawa Couplings in Higgs Searches at Tevatron and LHC

E. Gabrielli^a and B. Mele^b

^a *CERN, PH-TH, CH-1211 Geneva 23, Switzerland*

^b *INFN, Sezione di Roma, c/o Dip. di Fisica, Università di Roma “La Sapienza”,
Piazzale A. Moro 2, I-00185 Rome, Italy*

Abstract

We explore the possibility that, while the Higgs mechanism provides masses to the weak-gauge bosons at the electroweak scale as in the standard model, fermion masses are generated by an unknown mechanism at a higher energy scale. At low energies, the standard model can then be regarded as an effective field theory, where fermion masses explicitly break the electroweak $SU(2)_L \times U(1)_Y$ gauge symmetry. If Λ is the renormalization scale where the renormalized Yukawa couplings vanish, then at energies lower than Λ , effective Yukawa couplings will be radiatively induced by nonzero fermion masses. In this scenario, Higgs-boson decays into photons and weak gauge-bosons pairs are in general quite enhanced for a light Higgs. However, depending on Λ , a substantial decay rate into $b\bar{b}$ can arise, that can be of the same order as, or larger than, the *enhanced* $H \rightarrow \gamma\gamma$ rate. A new framework for Higgs searches at hadron colliders is outlined, vector-boson fusion becoming the dominant production mechanism at the CERN LHC, with an important role also played by the WH/ZH associated production. A detailed analysis of the Higgs branching fractions and their implications in Higgs searches is provided, versus the energy scale Λ .

1 Introduction

Arguably, one of the most intriguing aspects of particle physics is the origin of fermion masses. Despite the impressive phenomenological success of the standard model (SM) [1], a clear understanding of the fermion mass spectrum is still missing. The Higgs mechanism alone does not provide any explanation for the observed huge hierarchy in the fermion masses, that, not including the neutrino sector, ranges over 6 orders of magnitude. The Higgs Yukawa couplings, responsible for fermion-mass generation in the SM, are put in by hand, and tuned with the corresponding fermion masses times the inverse of the vacuum expectation value of the Higgs field. It is a matter of fact that, out of 19 free parameters of the SM, 13 belong to the Yukawa sector. This suggests that some new physics beyond the SM might be responsible for fermion masses and/or the flavor structure in the Yukawa couplings. Many extensions of the SM have been proposed to solve this puzzle, but none of them can be considered as conclusive.

A nonzero fermion mass explicitly breaks the chiral symmetry, and therefore the electroweak (EW) gauge symmetry $SU(2)_L \times U(1)_Y$. However, while the EW gauge symmetry breaking is needed for giving masses to the weak-gauge bosons, its mechanism could be different from the one responsible for the generation of fermion masses. In the SM there is only one mass scale: the vacuum expectation value v of the Higgs fields ($v \simeq 246$ GeV), which sets masses for both fermions and gauge bosons. On the other hand, the fermion mass generation scale could in principle be different from the EW symmetry breaking scale [2].

Once the Higgs boson is discovered at the CERN Large Hadron Collider (LHC), the analysis of its decay modes and production processes will help to unravel the mechanisms for both EW symmetry breaking and fermion mass generation (see, e.g., [3]). Direct Higgs boson searches at CERN LEP have excluded Higgs masses up to 114.4 GeV at 95% C.L. [4], while the Tevatron at Fermilab has recently ruled out the mass range $163 \text{ GeV} < m_H < 166 \text{ GeV}$ at 95% C.L. [5]. Moreover, indirect constraints on the Higgs boson mass and couplings come from the analysis of its virtual contributions to the EW processes. These contributions are not extremely sensitive to the Higgs boson mass, since, due to the decoupling theorem, one-loop radiative corrections depend only logarithmically on the Higgs mass. Nevertheless, electroweak precision tests (EWPT) point to a Higgs mass quite close to the LEP2 direct bound of 114.4 GeV. In particular, one gets an upper limit $m_H \leq 157 \text{ GeV}$ at 95% C.L., that can be relaxed up to $m_H \leq 186 \text{ GeV}$, if combined with the direct limit $m_H > 114.4 \text{ GeV}$ [6].

On the contrary, present EWPT do not really constrain Yukawa couplings. In fact, radiative corrections induced by Yukawa couplings of light fermions are tiny in the SM. Also, the SM Yukawa coupling contribution to the $Zb\bar{b}$ vertex is by far too small to be tested. The effects of the top-quark Yukawa corrections could be potentially large. On the other hand, in processes

with external light quarks or leptons, they enter only at two loops, which is beyond the present experimental sensitivity.

Flavor-changing neutral current (FCNC) processes generated at one loop in the SM are an excellent probe of the fermion mass-matrix structure, but they are weakly affected by the Yukawa corrections, too. The latter enter at the two-loop level, since no Higgs-boson exchange is needed at one loop to cancel the ultraviolet (UV) divergencies*. Even though fermion masses were put in by hand in the SM Lagrangian, due to the Glashow-Iliopoulos-Maiani mechanism [7], the FCNC processes would turn out to be finite at one loop with no need of Higgs-boson exchange between fermions†.

By the way, even gauge-couplings unification in grand unified theories (GUT) is weakly affected by Yukawa radiative corrections, since their contribution enters at the two-loop level in the renormalization group (RG) equations of gauge-couplings [8].

In conclusion, the fact that present experimental data do not significantly constrain Yukawa couplings still leaves room to speculations on the Higgs couplings to fermions, and eventually on the origin of fermion masses.

Following these considerations, we will explore the possibility that there is indeed a light Higgs boson that is mainly responsible for the EW symmetry breaking, but the chiral-symmetry breaking (ChSB) has a different origin. In particular, the conjecture explored in the present paper is the one where the (unavoidable) contribution of ChSB to the gauge boson masses is negligible with respect to the contribution provided by the Higgs boson. We will also assume that all the new physics effects responsible for the fermion mass generation can be reabsorbed in the nonvanishing fermion masses plus the renormalization conditions of the Yukawa couplings at a large energy scale Λ .

In order to implement the decoupling of the Higgs boson to standard fermions, we define Λ as the renormalization scale where the renormalized Yukawa couplings vanish. In general, Λ might not necessarily coincide with the scale of fermion mass generation.

We will also conservatively assume that potential new heavy degrees of freedom will not significantly affect the running of gauge and (effective) Higgs Yukawa couplings at high energies. Hence, from the EW scale up to the Λ scale, the SM can be regarded as an effective field theory, where the fermion mass terms explicitly break the $SU(2)_L$ gauge symmetry. Because of the presence of fermion mass terms, the decoupling of the Higgs boson from fermions is

*This is not true in the case of the so-called flavor-changing Higgs penguin diagrams, where a Higgs-boson is exchanged between a flavor-conserving current and a flavor-changing one induced at one-loop. However, this contribution to low-energy FCNC processes is tiny, being suppressed by the Yukawa couplings to the external light quarks.

†This is not true at the two-loop level, where Higgs boson exchange is necessary to cancel the UV divergencies.

spoiled at energy scales different from Λ . Because of the breaking of chiral symmetry, Yukawa couplings are not protected against radiative corrections, and effective Yukawa couplings will be radiatively induced at low energies.

In this article, we will evaluate the effective Yukawa couplings at energies lower than Λ , by the techniques of RG equations. This will allow us to resum the leading logarithmic terms $g_i^{2n} \log^n (\Lambda/m_H)$ (where g_i are the SM gauge couplings), at any order in perturbation theory.

We will explicitly check that contributions from higher-dimensional operators, that could spoil the validity of perturbation theory in the Yukawa sector, are well under control for any value of Λ up to the GUT scale (10^{16}GeV), provided the Higgs mass is not much larger than the EW scale v . A critical discussion on the validity of our approach for large values of Λ will be provided in the next sections. In our analysis we will set the upper value of Λ at the GUT scale, which guarantees the perturbativity of the Yukawa sector in all the Λ range for $m_H < v$. Nevertheless, the existing models that could provide a specific UV completion to our effective theory are in general characterized by a Λ scale much lower than 10^{16} GeV .

The present model differs substantially from the fermiophobic Higgs boson scenario, appearing in several extensions of the SM [9]. Indeed, we will see that the Higgs boson decay rate into $b\bar{b}$ can be strongly enhanced at low energy, depending on the size of Λ . In the fermiophobic Higgs scenario, the Higgs couplings to fermions are set to zero at the EW scale $\Lambda_{\text{EW}} \sim m_H$. This condition can naturally arise within new physics models where the scale Λ is not far from the EW scale. In our approach, when $\Lambda \rightarrow m_H$, all the leading-log terms $\log^n (\Lambda/m_H)$, as well as the renormalization effects on the Yukawa couplings at the EW scale, vanish. One then smoothly recovers the fermiophobic Higgs model.

Note that the suppression of the top Yukawa coupling in the present approach somewhat relieves the SM hierarchical problem in the one-loop radiative corrections to the Higgs mass (see, e.g., [2]), where the dominant contribution to the quadratic cut-off dependence is now the one of order $\mathcal{O}(M_W^2)$ instead of $\mathcal{O}(m_t^2)$.

A straightforward way to test our scenario for $m_H \lesssim 150\text{ GeV}$ is through the measurement of Higgs boson decay and production rates at colliders. The vanishing of the top-quark Yukawa coupling at tree-level has a dramatic impact on the Higgs boson production at hadron colliders. The vector boson fusion (VBF) [10, 11, 12] will replace the gluon fusion via the top-quark loop [13, 14] as the main production mechanism at the LHC. If the Higgs boson is quite light, as suggested by EWPT, the dominant Higgs decays channels will be into WW , ZZ (where one of the weak gauge bosons, or both, can be off-shell), and $\gamma\gamma$. The rate for $H \rightarrow b\bar{b}$ will turn out to be comparable to the $H \rightarrow \gamma\gamma$ rate at $\Lambda \sim 10\text{ TeV}$, while it increases at larger Λ 's. Furthermore, the enhanced branching ratio $\text{BR}(H \rightarrow \gamma\gamma)$ makes the WH/ZH associated production with $H \rightarrow \gamma\gamma$ a remarkably interesting channel that could be studied for inclusive W/Z decays.

Present direct experimental limits on m_H crucially depend on the SM Yukawa coupling assumption. Bounds on m_H in the purely fermiophobic Higgs scenario have been obtained at LEP, where one finds $m_H > 109.7$ GeV at 95% C.L. [15], and the Tevatron, where the D0 experiment provides a limit $m_H > 101$ GeV at 95% C.L.[16] and the CDF experiment gives a bound $m_H > 106$ GeV at 95% C.L.[17]. In the framework we are going to discuss, non trivial variations in the Higgs decay pattern are expected with respect to the fermiophobic scenario that would require a new analysis of experimental data in order to get dedicated bounds on m_H , depending on the scale Λ .

The paper is organized as follows. In Sec. 2, we present the theoretical framework, derive the RG equations for the effective Yukawa couplings, and give some numerical results for the latter. After a few comments on the theoretical consistency of the present approach, discussed in Sec. 3, we provide, in Sec. 4, the numerical results for the Higgs branching ratios, as a function of the energy scale Λ . In Sec. 5, we study Higgs production rates corresponding to different decay signatures at hadronic colliders. Our conclusions will be presented in Sec. 6. In the Appendix, we supply relevant formulas for the Higgs boson decays.

2 RG equations for effective Yukawa couplings

In this section, we will derive the RG equations for the effective Yukawa couplings arising from the conjecture that the standard Higgs mechanism provides masses to the weak gauge-bosons at the EW scale, while fermion masses are not generated by Yukawa couplings as in the SM framework. We will assume that from the EW scale up to some larger energy scale, only SM degrees of freedom are relevant, and fermion masses are put in by hand. Since by switching off the SM tree-level couplings of the Higgs-boson to fermions, the SM becomes nonrenormalizable, we should consider it as an effective field theory valid up to some high-energy scale.[‡]

Let us define the relevant EW Lagrangian in the unitary gauge, with only physical degrees of freedom propagating

$$\mathcal{L} = \mathcal{L}_{G,H} + \mathcal{L}_F. \quad (1)$$

$\mathcal{L}_{G,H}$ is the bosonic sector of the SM EW Lagrangian in the unitary gauge, containing the gauge fields $G = \{A_\mu, W_\mu^\pm, Z_\mu\}$, and A and H are the photon and Higgs fields respectively. \mathcal{L}_F

[‡] Notice that one can always introduce in the Lagrangian fermion mass terms without Yukawa couplings in a $SU(2) \times U(1)_Y$ gauge-invariant way by considering the nonlinear realization of the EW gauge symmetry. Also in this case, the theory is manifestly nonrenormalizable.

regards the fermionic sector of the Lagrangian

$$\mathcal{L}_F = \mathcal{L}_{Kin} + \mathcal{L}_{CC} + \mathcal{L}_{NC} - \frac{1}{\sqrt{2}} \sum_f Y_f (\bar{\psi}_f \psi_f H) - \sum_f m_f \bar{\psi}_f \psi_f, \quad (2)$$

where \mathcal{L}_{Kin} is the kinetic term, \mathcal{L}_{CC} and \mathcal{L}_{NC} are the SM Lagrangian for the charged- and neutral-currents interactions of quarks and leptons, and Y_f are the Yukawa couplings, in the basis of fermion mass eigenstates. In eq. (2), we neglect the CKM mixing, since we are interested in flavor-conserving Higgs transitions. Hence, all parameters in eq. (2) are real.

The Lagrangian in eq. (2) is basically the SM one, where tree-level relations between fermion masses and Yukawa interactions have been relaxed. Yukawa couplings will be introduced in any case, since, after breaking the chiral symmetry explicitly through the fermion mass terms in eq. (2), they are no more protected against radiative corrections. Even assuming vanishing Yukawa couplings at tree level, divergent terms, proportional to fermion masses, will arise radiatively at loop level. The latter can only be canceled by counterterms proportional to the Yukawa-Higgs-fermion interactions. Therefore, the operators $(Y_f \bar{\psi}_f \psi_f H)$, even if not present in the classical Lagrangian, will reappear at the quantum level, due to the nonvanishing Dirac mass terms.

Starting from the effective Lagrangian in eqs.(1)-(2), new contributions to the β functions of Yukawa couplings are expected with respect to the SM results, due to the fact that m_f terms do not arise from spontaneous chiral symmetry breaking. Since the theory is not renormalizable, the off shell renormalization of the Yukawa operator $O_{Y_f} = \bar{\psi}_f \psi_f H$ implies in general higher-dimensional counterterms, like for instance $\sim (\partial_\mu \bar{\psi}_f)(\partial^\mu \psi_f) H$, introducing new coupling constants. However, since here we are interested in *on shell* Higgs coupling to fermions (that are relevant, e.g., in Higgs boson decays), the Yukawa operator O_{Y_f} will be renormalized by evaluating one-loop matrix elements with all external legs *on shell*. Then, as can be checked by explicit calculation, all the divergencies can be reabsorbed in Yukawa couplings and field renormalization constants. This is no more true when the Higgs field is off shell, and the contribution from the mixing of *off shell* higher-dimensional operators is to be taken into account in the renormalization of Yukawa couplings. Notice that this discussion does not apply to the SM, which is a renormalizable theory.

The relevant β function will be worked out through the usual steps. First, one has to derive the relation between the bare (Y_f^0) and the renormalized (Y_f) Yukawa couplings (where f refers to a generic fermion field). In general, one has

$$Y_f^0 = Z_{Y_f} Z_{\psi_f}^{-1} Z_H^{-1/2} Y_f. \quad (3)$$

As usual, the symbol Z_{Y_f} is the renormalization constant canceling the divergencies associated to the *one-particle irreducible* matrix elements of the Yukawa operator O_{Y_f} , while the terms

Z_{ψ_f} and Z_H are the wave-function renormalization constants of the f fermion and Higgs fields, respectively. Neglecting the contributions to the β function induced by the CKM mixing in the one-loop calculation, the renormalization constants, as well as the bare and renormalized Yukawa couplings, will be diagonal matrices in the flavor space.

We perform the one-loop integrals in D -dimensions, with $D = 4 - \epsilon$, and subtract the divergent part by using the $\overline{\text{MS}}$ renormalization scheme. In dimensional regularization, the bare Yukawa coupling Y_f^0 can be expressed as a Laurent series in ϵ

$$Y_f^0 = \mu^{\epsilon/2} \left(Y_f + \sum_{n=1}^{\infty} \frac{a_{nf}(Y_f, g_i)}{\epsilon^n} \right), \quad (4)$$

where μ is the renormalization scale as defined in the $\overline{\text{MS}}$ scheme, and g_i , with $i = 1, 2, 3$, indicate the SM gauge coupling constants associated to the $\text{SU}(3)_c \times \text{SU}(2)_L \times \text{U}(1)_Y$ gauge group. In eq.(4) we have omitted the dependence on the renormalization scale μ in the (renormalized) Yukawa couplings and gauge couplings g_i . Notice that the coefficients $a_{nf}(Y_f, g_i)$ in eq.(4) depend on μ through the μ dependence of both the renormalized Yukawa and gauge couplings.

As usual, the Yukawa β function is defined as $\beta_{Y_f} = dY_f/dt$, with $t = \log \mu$, and is connected to the residue of the simple pole $1/\epsilon$ in eq.(4), that is to $a_{1f}(Y_f, g_i)$. Then, according to the notation in eq.(4), one obtains

$$\beta_{Y_f} = \frac{1}{2} \left(-1 + \sum_{f'} Y_{f'} \frac{\partial}{\partial Y_{f'}} + \sum_{i=1}^3 g_i \frac{\partial}{\partial g_i} \right) a_{1f}(Y_f, g_i), \quad (5)$$

where the sum on f' runs over all the nonvanishing fermion contributions.

The full set of the one-loop diagrams contributing (in the unitary gauge for the W and Z propagators, and with the CKM matrix set to unity) to the term a_{1f} in eq.(4) is given in Fig.1 for the up-type quarks $U = \{u, c, t\}$. (The case of down-type quarks $D = \{d, s, b\}$ and charged leptons $E = \{e, \mu, \tau\}$ can be obtained from Fig.1 in a straightforward way.) Diagrams in Figs. 1(a)-1(e) correspond to the vertex corrections, while Figs. 1(f)-1(g) and 1(h)-1(k) are the self-energy corrections to the Higgs boson and up-type quark fields, respectively. The vertex correction with two internal Higgs boson lines, and the Higgs self-energy diagram with a Higgs boson loop have not been included in Fig.1. Indeed, this vertex correction and the contribution to the Higgs wave-function renormalization arising from the Higgs-boson loop are finite, and so do not contribute to the β function.

The RG equations for the effective Yukawa couplings at one-loop are then given by

$$\begin{aligned} \frac{d\mathbf{Y}_U}{dt} &= \frac{1}{16\pi^2} \left\{ 3\xi_H^2 (\mathbf{Y}_U - \mathbf{Y}_U^{\text{SM}}) - 3\mathbf{Y}_U^{\text{SM}} \mathbf{Y}_D^{\text{SM}} (\mathbf{Y}_D - \mathbf{Y}_D^{\text{SM}}) + \frac{3}{2} \mathbf{Y}_U (\mathbf{Y}_U \mathbf{Y}_U - \mathbf{Y}_D^{\text{SM}} \mathbf{Y}_D^{\text{SM}}) \right. \\ &\quad \left. - \mathbf{Y}_U \left(\frac{17}{20} g_1^2 + \frac{9}{4} g_2^2 + 8g_3^2 - \text{Tr}(\mathbf{Y}) \right) \right\}, \end{aligned} \quad (6)$$

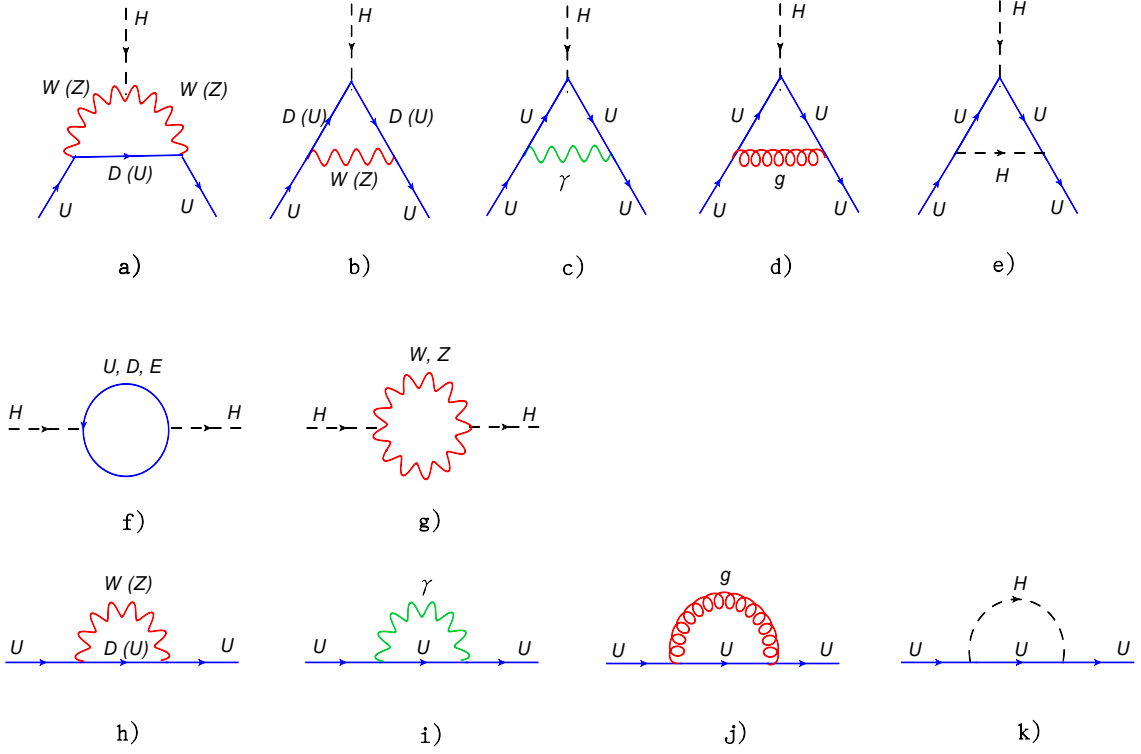


Figure 1: One-loop Feynman diagrams contributing, in the unitary gauge, to the β function of the Yukawa couplings of up-type quarks $U = \{u, c, t\}$. Labels γ and g correspond to the photon and gluon propagators, respectively. Diagrams in Figs. 1(a)-1(e) refer to the vertex corrections, while 1(f)-1(g) and 1(h)-1(k) refer to the Higgs boson H and the up-type quarks' self-energy corrections, respectively. The labels $D = \{d, s, b\}$ and $E = \{e, \mu, \tau\}$ stand for the down-type quarks and charged leptons, respectively.

$$\begin{aligned} \frac{d\mathbf{Y}_D}{dt} &= \frac{1}{16\pi^2} \left\{ 3\xi_H^2 (\mathbf{Y}_D - \mathbf{Y}_D^{\text{SM}}) - 3\mathbf{Y}_D^{\text{SM}} \mathbf{Y}_U^{\text{SM}} (\mathbf{Y}_U - \mathbf{Y}_U^{\text{SM}}) + \frac{3}{2} \mathbf{Y}_D (\mathbf{Y}_D \mathbf{Y}_D - \mathbf{Y}_U^{\text{SM}} \mathbf{Y}_U^{\text{SM}}) \right. \\ &\quad \left. - \mathbf{Y}_D \left(\frac{1}{4} g_1^2 + \frac{9}{4} g_2^2 + 8g_3^2 - \text{Tr}(\mathbf{Y}) \right) \right\}, \end{aligned} \quad (7)$$

$$\frac{d\mathbf{Y}_E}{dt} = \frac{1}{16\pi^2} \left\{ 3\xi_H^2 (\mathbf{Y}_E - \mathbf{Y}_E^{\text{SM}}) + \frac{3}{2} \mathbf{Y}_E \mathbf{Y}_E \mathbf{Y}_E - \mathbf{Y}_E \left(\frac{9}{4} (g_1^2 + g_2^2) - \text{Tr}(\mathbf{Y}) \right) \right\}, \quad (8)$$

where Tr stands for the trace, and the matrix \mathbf{Y} is defined as

$$\mathbf{Y} \equiv N_c \mathbf{Y}_U \mathbf{Y}_U + N_c \mathbf{Y}_D \mathbf{Y}_D + \mathbf{Y}_E \mathbf{Y}_E. \quad (9)$$

In the above equations, we used the notation $\mathbf{Y}_{U,D,E}$ for the Yukawa couplings, that stands for

diagonal 3×3 real matrices in flavor space (where $\mathbf{U}, \mathbf{D}, \mathbf{E}$ stand for up-quarks, down-quarks and charged leptons, respectively). Then, products of $\mathbf{Y}_{\mathbf{U}, \mathbf{D}, \mathbf{E}}$ are understood in the matrix space. The remaining symbols in eqs.(6)-(8) are defined as

$$\xi_H \equiv \frac{g_2 m_H}{2M_W}, \quad \mathbf{Y}_{\mathbf{f}}^{\text{SM}} \equiv \frac{g_2}{\sqrt{2}M_W} \text{diag}[m_{f_1}, m_{f_2}, m_{f_3}], \quad g_1^2 \equiv \frac{5}{3} \frac{e^2}{\cos^2 \theta_W}, \quad (10)$$

where $\mathbf{Y}_{\mathbf{f}}^{\text{SM}}$ is a diagonal matrix in flavor space, m_{f_i} being the fermion pole-masses, with $\mathbf{f} = \mathbf{U}, \mathbf{D}, \mathbf{E}$, and $N_c = 3$ the number of colors. The RG equations for the gauge couplings are the same as in the SM[8]

$$\frac{dg_i}{dt} = -b_i \frac{g_i^3}{16\pi^2}, \quad (11)$$

with

$$\begin{aligned} b_1 &= -\frac{4}{3}n_g - \frac{1}{10}, \\ b_2 &= \frac{22}{3} - \frac{4}{3}n_g - \frac{1}{6}, \\ b_3 &= 11 - \frac{4}{3}n_g, \end{aligned}$$

and $n_g = 3$ is the number of fermion generations. The parameters $\mathbf{Y}_{\mathbf{f}}^{\text{SM}}$ in eq.(10) are the explicit chiral-symmetry breaking parameters, that depend on the running scale $t = \log \mu$ through the weak-gauge coupling $g_2(t)$. They coincide with the tree-level SM Yukawa couplings. Vertex and self-energies diagram contributions entering in eqs.(6)-(8) have been cross-checked with the SM results for the unitary gauge in [18].

We stress that $\mathbf{Y}_{\mathbf{f}}^{\text{SM}}$ in eqs.(6)-(8) is kept independent from the Yukawa couplings. For $\mathbf{Y}_{\mathbf{f}}^{\text{SM}} \rightarrow \mathbf{Y}_{\mathbf{f}}$, the Higgs mechanism for the fermion mass generation, and the corresponding SM RG equations [8] are recovered.

Another interesting limit is when all the Yukawa couplings are set to zero at some scale. Then, the diagrams with two W and two Z exchange in the loop [cf. Fig.1(a)] give the leading contribution to the β function, since they are both divergent in the unitary gauge. Indeed, in the limit $\mathbf{Y}_{\mathbf{f}} \rightarrow 0$, the β functions are nonvanishing, and the leading contribution is proportional to corresponding fermion mass times the Higgs mass squared

$$\beta_{\mathbf{Y}_{\mathbf{U}}}(\mathbf{Y}_{\mathbf{f}} \rightarrow 0) = -\frac{3\mathbf{Y}_{\mathbf{U}}^{\text{SM}}}{16\pi^2} \left(\xi_H^2 - (\mathbf{Y}_{\mathbf{D}}^{\text{SM}})^2 \right), \quad (12)$$

$$\beta_{\mathbf{Y}_{\mathbf{D}}}(\mathbf{Y}_{\mathbf{f}} \rightarrow 0) = -\frac{3\mathbf{Y}_{\mathbf{D}}^{\text{SM}}}{16\pi^2} \left(\xi_H^2 - (\mathbf{Y}_{\mathbf{U}}^{\text{SM}})^2 \right), \quad (13)$$

$$\beta_{\mathbf{Y}_{\mathbf{E}}}(\mathbf{Y}_{\mathbf{f}} \rightarrow 0) = -\frac{3\mathbf{Y}_{\mathbf{E}}^{\text{SM}}}{16\pi^2} \xi_H^2. \quad (14)$$

The structure of the r.h.s. of eqs.(12)-(14) is crucial to radiatively induce effective Yukawa couplings at low energy. Indeed, due to the *explicit* breaking of chiral symmetry by fermion masses, the right-hand side of eqs.(6)-(8) does not vanish in the $\mathbf{Y}_f \rightarrow 0$ limit. Hence, Yukawa couplings receive radiative logarithmic contributions at low energy, even if they are vanishing at some high-energy scale.

The appearance of terms proportional to $\xi_H^2 \sim m_H^2/M_W^2$ in the right-hand side of eqs.(6)-(8) can be interpreted as a manifestation of the nonrenormalizability of the theory. These terms come from the divergent part of the vertex diagrams with two W or two Z running in the loop [cf. Fig.1(a)], and from the W and Z loop contribution to the Higgs self-energy diagram [cf. Fig.1(g)]. Their contribution vanishes when $\mathbf{Y}_f^{\text{SM}} \rightarrow \mathbf{Y}_f$ in eqs.(6)-(8). When considering the renormalization of the Yukawa operator with an *off-shell* Higgs field, an analogous divergent term proportional to the Higgs-momentum square q^2 will appear from the same diagrams. This term can be reabsorbed in the renormalization of the dimension-6 operator $\sim (\partial_\mu \bar{\psi}_f)(\partial^\mu \psi_f)H$, that explicitly breaks the renormalizability of the theory. In general, due to the nonrenormalizability of the effective theory, at higher orders in perturbation theory we expect new contributions to the beta-function proportional to higher powers of q^2/M^2 , where M is an effective scale (inversely proportional to the fermion masses), that is about 3 TeV for the top-quark case, and much higher for the lighter fermions [cf. eqs.(6)-(8), when $m_H^2 \sim q^2$]. Therefore, if we assume that the characteristic energy of the process (that, in Higgs decays, is $q^2 = m_H^2$) is well below this scale, higher-order effects coming from the truncation of the perturbative series can be safely neglected. Clearly, this statement is automatically fulfilled for the light Higgs boson scenario, where $m_H \leq 150$ GeV.

In order to connect the Yukawa couplings $Y_f(m_H)$ at the low energy scale m_H with their values $Y_f(\Lambda)$ at some high-energy scale Λ , we will numerically integrate the RG equations in eqs.(6)-(8) from $\mu = \Lambda$ down to $\mu = m_H$. The actual solution will depend on the choice of boundary conditions for the Yukawa couplings $Y_f(\Lambda)$, while for the gauge couplings we assume as input their experimental central values at the scale M_Z .

We define Λ as the renormalization scale where all the Yukawa couplings vanish[§]. This choice is motivated by the present guess that the Higgs mechanism is decoupled from the chiral-symmetry-breaking mechanism at some high-energy scale. In principle, the condition of

[§]Notice that in the SM this condition would have trivial implications. Indeed, due to the Higgs mechanism, if the Yukawa couplings (and hence fermion mass parameters) are set to zero at some renormalization scale, they would be zero also at any other scale, and fermion mass terms would not be generated. Moreover, the fact that all the Yukawa are required to vanish at the same scale follows from some sort of flavor universality in the mechanism of fermion mass generation

vanishing Yukawa couplings at the scale Λ could seem an oversimplification, when considered in the framework of a realistic NP model that could explain the fermion-mass generation above the scale Λ . Indeed, since Yukawa couplings should vanish in the limit $m_f \rightarrow 0$, one expects, on dimensional grounds, a suppression $Y_f(\Lambda) \sim \mathcal{O}(m_f/\Lambda)$, in case the fermion mass parameters are the only chiral-symmetry-breaking parameters of the theory[¶]. Then it is straightforward to check that, if Λ is a few orders of magnitude above the EW scale, the solution of the RG equations with $Y_f(\Lambda) \sim \mathcal{O}(m_f/\Lambda)$ is well approximated by vanishing boundary conditions for the Yukawa couplings.

Because of the term proportional to $\xi_H^2 \sim m_H^2/M_W^2$ in eq.(12), for large m_H , the renormalized top Yukawa coupling $Y_t(m_H)$, evaluated at the scale $\mu = m_H$, could become very large due to RG equation effects, and could spoil the perturbative approach in the Yukawa sector. The requirement that the top Yukawa coupling does not exceed unity at the EW scale can be translated into an upper bound on the Higgs boson mass as a function of Λ . In particular, if we retain only the leading contribution in the β function of the top Yukawa coupling, the RG equation in eq.(6) becomes

$$\frac{dY_t}{dt} \simeq -\frac{3}{16\pi^2} \xi_H^2 (Y_t - Y_t^{\text{SM}}). \quad (15)$$

Equation (15) can be easily solved in the approximation of assuming $g_2(t)$ as a constant. Setting the $g_2(t)$ value at the M_Z scale, by requiring $Y_t(M_Z) < 1$, one then obtains the following upper bound on the Higgs mass

$$m_H < 2\pi \sqrt{\log\left(\frac{1 + Y_t^{\text{SM}}}{Y_t^{\text{SM}}}\right) \frac{2\sqrt{2}}{3 G_F \log(\frac{\Lambda}{M_Z})}}. \quad (16)$$

Equation (16) sets up the m_H range, versus Λ , where perturbation theory in the Yukawa sector can be still reliable in the present scenario. The numerical values of the upper bounds obtained from eq.(16) are $m_H^{\text{max}} \simeq 687, 488, 346, 261$ GeV, for $\Lambda = 10^{\{4,6,10,16\}}$, respectively. These bounds are rather stronger than the ones derived from the exact solution of top-Yukawa eq.(6) evaluated at the m_H scale. In particular, the exact m_H bounds for $Y_t(m_H) < 1$ are $m_H^{\text{max}} \simeq \{611, 443, 366\}$ GeV, for $\Lambda = 10^{\{6,10,16\}}$ GeV, respectively, while for $\Lambda = 10^4$ GeV, there is basically no upper limits (below 1 TeV) on the Higgs mass. The latter bounds can also be worked out from Fig.2, where we plot, versus m_H and for different Λ 's in the range 10^4 – 10^{16} GeV, the effective Yukawa couplings of bottom and top quarks, evaluated at the $\mu = m_H$ scale, and normalized to their tree-level SM values.

Figure 2 also shows that for $m_H \sim (100\text{--}250)$ GeV, the absolute value of the b quark effective Yukawa coupling decreases when m_H increases, and vanishes in the range $m_H \simeq (250 - 275)$

[¶]Different scenarios could also be envisaged.

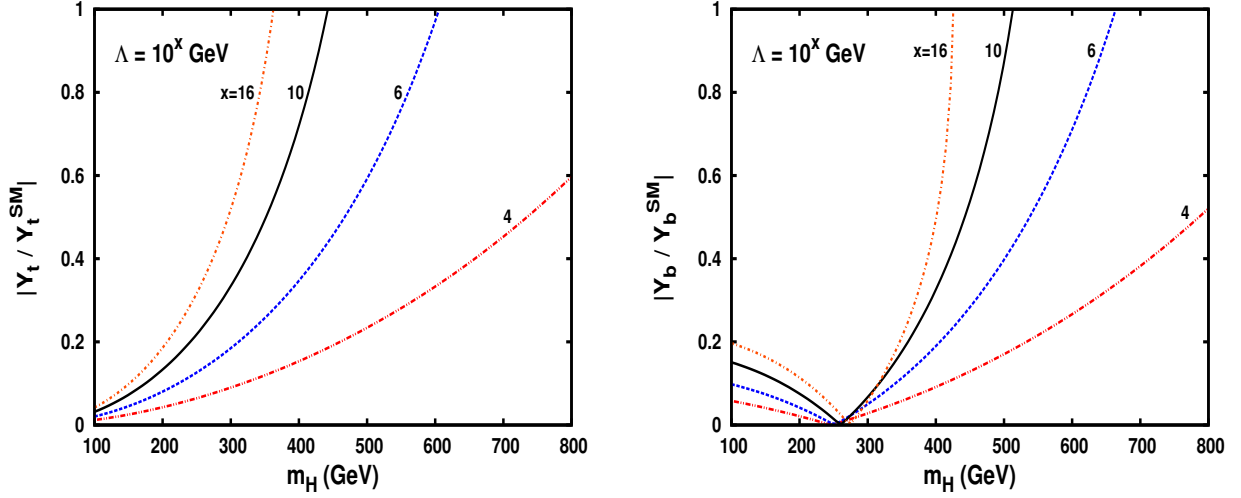


Figure 2: Absolute values of the effective Yukawa couplings for top quarks (left) and bottom quarks (right), $|Y_f(m_H)/Y_f^{\text{SM}}|$, evaluated at the m_H scale, and normalized to their respective tree-level SM values, versus m_H , and for different Λ 's. We assume $Y_t^{\text{SM}} = 0.997$ and $Y_b^{\text{SM}} = 0.0284$, corresponding, respectively, to the pole masses $m_t=171.3$ GeV and $m_b=4.88$ GeV, and $g_2 = g_2(M_Z)$ in eq.(10).

GeV, the exact m_H value depending on Λ . The effective top-Yukawa coupling is always negative for $m_H > 100$ GeV, while the bottom-Yukawa coupling is positive (negative) for values of the Higgs mass below (above) the minimum of its absolute value.

In Table 1, we present the values of the effective Yukawa couplings for t, b, c quarks and τ, μ leptons, as obtained by numerically solving eqs.(6)-(8), versus m_H , and for $\Lambda = 10^{4,6,10,16}$ GeV. For reference, the corresponding Yukawa-coupling SM values [defined as in eq.(10), with $g_2 = g_2(M_Z)$], are given by $Y_t^{\text{SM}} = 0.997$, $Y_b^{\text{SM}} = 0.0284$, $Y_c^{\text{SM}} = 9.54 \cdot 10^{-3}$, $Y_\tau^{\text{SM}} = 0.0103$, $Y_\mu^{\text{SM}} = 6.15 \cdot 10^{-4}$. One can see that effective bottom Yukawa coupling is of the order 10% of Y_b^{SM} , in the m_H and Λ ranges considered.

Table 1 also shows that the top-quark Yukawa coupling is at most $\mathcal{O}(10^{-2}) - \mathcal{O}(10^{-1})$, for $m_H \simeq (100 - 160)$ GeV. Then, in Higgs boson production at hadron colliders, the gluon fusion turns out to be quite depleted with respect to the VBF mechanism. For larger m_H (cf. Fig.2), the top Yukawa coupling increases, and the cross section for gluon fusion can still be competitive, and even larger than the VBF cross section.

In the following sections, after a few comments on the theoretical consistency of the present approach, we will discuss the phenomenological implications of the present results.

$m_H(\text{GeV})$	$\Lambda(\text{GeV})$	$ Y_t(m_H) $	$ Y_b(m_H) $	$ Y_c(m_H) $	$ Y_\tau(m_H) $	$ Y_\mu(m_H) $
100	10^4	1.2×10^{-2}	1.6×10^{-3}	1.2×10^{-4}	1.4×10^{-4}	8.5×10^{-6}
	10^6	2.0×10^{-2}	2.8×10^{-3}	2.0×10^{-4}	2.7×10^{-4}	1.6×10^{-5}
	10^{10}	3.2×10^{-2}	4.3×10^{-3}	3.0×10^{-4}	4.7×10^{-4}	2.8×10^{-5}
	10^{16}	4.2×10^{-2}	5.6×10^{-3}	4.0×10^{-4}	7.0×10^{-4}	4.2×10^{-5}
110	10^4	1.4×10^{-2}	1.6×10^{-3}	1.4×10^{-4}	1.7×10^{-4}	1.0×10^{-5}
	10^6	2.5×10^{-2}	2.7×10^{-3}	2.4×10^{-4}	3.2×10^{-4}	1.9×10^{-5}
	10^{10}	3.8×10^{-2}	4.1×10^{-3}	3.7×10^{-4}	5.7×10^{-4}	3.4×10^{-5}
	10^{16}	5.1×10^{-2}	5.4×10^{-3}	4.9×10^{-4}	8.5×10^{-4}	5.1×10^{-5}
120	10^4	1.7×10^{-2}	1.5×10^{-3}	1.6×10^{-4}	2.0×10^{-4}	1.2×10^{-5}
	10^6	2.9×10^{-2}	2.5×10^{-3}	2.8×10^{-4}	3.8×10^{-4}	2.3×10^{-5}
	10^{10}	4.6×10^{-2}	4.0×10^{-3}	4.4×10^{-4}	6.8×10^{-4}	4.0×10^{-5}
	10^{16}	6.1×10^{-2}	5.3×10^{-3}	5.9×10^{-4}	1.0×10^{-3}	6.1×10^{-5}
130	10^4	1.9×10^{-2}	1.4×10^{-3}	1.9×10^{-4}	2.3×10^{-4}	1.4×10^{-5}
	10^6	3.4×10^{-2}	2.4×10^{-3}	3.3×10^{-4}	4.4×10^{-4}	2.6×10^{-5}
	10^{10}	5.4×10^{-2}	3.8×10^{-3}	5.2×10^{-4}	8.0×10^{-4}	4.8×10^{-5}
	10^{16}	7.2×10^{-2}	5.1×10^{-3}	6.9×10^{-4}	1.2×10^{-3}	7.2×10^{-5}
140	10^4	2.2×10^{-2}	1.3×10^{-3}	2.1×10^{-4}	2.6×10^{-4}	1.6×10^{-5}
	10^6	3.9×10^{-2}	2.3×10^{-3}	3.8×10^{-4}	5.1×10^{-4}	3.0×10^{-5}
	10^{10}	6.3×10^{-2}	3.6×10^{-3}	6.0×10^{-4}	9.3×10^{-4}	5.5×10^{-5}
	10^{16}	8.5×10^{-2}	4.9×10^{-3}	8.1×10^{-4}	1.4×10^{-3}	8.4×10^{-5}
150	10^4	2.5×10^{-2}	1.2×10^{-3}	2.4×10^{-4}	3.0×10^{-4}	1.8×10^{-5}
	10^6	4.5×10^{-2}	2.1×10^{-3}	4.3×10^{-4}	5.9×10^{-4}	3.5×10^{-5}
	10^{10}	7.3×10^{-2}	3.4×10^{-3}	7.0×10^{-4}	1.1×10^{-3}	6.4×10^{-5}
	10^{16}	9.8×10^{-2}	4.6×10^{-3}	9.4×10^{-4}	1.6×10^{-3}	9.8×10^{-5}
160	10^4	2.8×10^{-2}	1.1×10^{-3}	2.7×10^{-4}	3.3×10^{-4}	2.0×10^{-5}
	10^6	5.1×10^{-2}	1.9×10^{-3}	4.9×10^{-4}	6.7×10^{-4}	4.0×10^{-5}
	10^{10}	8.3×10^{-2}	3.2×10^{-3}	8.0×10^{-4}	1.2×10^{-3}	7.3×10^{-5}
	10^{16}	1.1×10^{-1}	4.4×10^{-3}	1.1×10^{-3}	1.9×10^{-3}	1.1×10^{-4}

Table 1: Absolute values of the effective Yukawa couplings for t, b, c quarks and τ, μ leptons, evaluated at the scale m_H , for different values of the Higgs mass and the energy scale Λ . The corresponding values of the SM Yukawa couplings Y_f^{SM} [as defined in eq.(10), with $g_2 = g_2(M_Z)$] are given by $Y_t^{\text{SM}} = 0.997$, $Y_b^{\text{SM}} = 0.0284$, $Y_c^{\text{SM}} = 9.54 \cdot 10^{-3}$, $Y_\tau^{\text{SM}} = 0.0103$, $Y_\mu^{\text{SM}} = 6.15 \cdot 10^{-4}$.

3 Possible open issues in the present theoretical model

Before proceeding to a more phenomenological study, we will comment on possible issues that could endanger the consistency of the present theoretical approach to the ChSB. In particular, we will address the issue of tree-level unitarity, the presence of a possible fine-tuning in the eventual UV completion of the theory, and the consistency of the model with EWPT.

One could wonder whether, by pushing apart the scales of the EW symmetry breaking and the fermion mass generation, problems with (perturbative) tree-level unitarity would arise [19]. Indeed, when fermion masses are put in by hand, the partial-wave unitarity in the tree-level fermion-antifermion scatterings into massive gauge bosons will be spoiled at some c.m. energy scale E_0 , which is proportional to the inverse of the fermion masses m_f , $E_0 \simeq \frac{4\pi\sqrt{2}}{\sqrt{3N_C}G_F m_f}$, where $N_C = 1(3)$ for leptons (quarks), and G_F is the Fermi constant [19]. Then, the corresponding unitarity bounds range from 3 TeV for the top-quark up to 1.7×10^6 TeV for the electron. In a more recent analysis [20], multiple massive gauge boson productions in fermion-antifermion scatterings has been considered, which provide even more stringent unitarity bounds for light fermions.

Let us now suppose that in the SM the scale of fermion mass generation is pushed above the scale of unitarity bounds. As recalled above, if we switch off the Higgs coupling to fermions, the SM becomes nonrenormalizable and perturbation theory ceases to be a good approximation for real processes involving energies above the scale of unitarity bounds. Unless we want to restore *perturbative* unitarity at all energies (which would call for new degrees of freedom with masses of the order of the scale of unitarity bounds), the interpretation of these bounds in terms of the scale of fermion mass generation will be questionable.

In our approach, the theory keeps consistent even at scales above unitarity bounds, although the validity of perturbation theory will of course be subject to restrictions. We will assume that unitarity will be recovered not by new fundamental massive particles, but, for instance, by new nonperturbative phenomena arising in scattering processes at energies above the scale of unitarity bounds. Regarding processes at energies below the scale of unitarity bounds (that we are concerned with in the present analysis), perturbation theory can still be trusted, provided the effects of potential higher-dimensional operators, connected to the nonrenormalizability of the theory, are under control, and do not spoil the perturbative expansion (as discussed in Section 2).

Next, in our approach we implicitly assume that a UV completion of the theory, that is free from fine-tuning problems, can be realized. In general, ChSB implies EWSB, while EWSB does not necessarily imply ChSB. Therefore, in case the scale of fermion-mass generation is taken arbitrarily large with respect to the W and Z mass scale, concerns about a potential fine-tuning

in the EWSB and ChSB contributions to the weak gauge-boson masses are legitimate. However, these expectations are natural only in case the mechanism of fermion mass generation is perturbative, or, analogously, the hidden sector responsible for ChSB is weakly coupled. There are examples in the literature, in the framework of nonperturbative ChSB mechanisms, where the aforementioned fine-tuning problem (or hierarchy problem) does not arise [21, 22, 23]. In the model in [21], a dynamical ChSB mechanism with large anomalous dimensions for the top-quark condensate is proposed, where the scale of ChSB can be as high as the Planck scale, while no fine-tuning in the W and Z masses at the EW scale are expected to arise. More exotic interactions involving, for instance, Lorentz-violating four-fermion operators suppressed by a scale above the GUT scale, have been conjectured in [22] to dynamically trigger ChSB at low energy.

An approach similar to our scenario has also been recently explored in the context of Technicolor models [24, 23]. In [23], a fundamental light Higgs is introduced to induce EWSB, while fermion masses are generated by extended-Technicolor interactions well above the EWSB scale.

Finally, in our effective theory, quadratic divergencies in the W and Z self-energies could in principle appear due to radiative corrections. Although the latter will be in general proportional to fermion masses, they could spoil the EWPT even for moderate values of Λ , in case the fermion mass involved is the top-quark mass. However, these corrections are not expected to arise at one loop, since Yukawa interactions are not entering the W and Z self-energies at this order. Indeed, at one loop the oblique corrections (S,T,U variables [25]) are not affected when switching from the SM to our model. At two loop, an estimate of oblique corrections is less straightforward. By a closer inspection of the superficial degree of divergency in the corresponding two-loop diagrams, we expect that terms proportional to the square of the cutoff Λ be absent, hence taming a potential tension in the EWPT for large Λ . This expectation is supported by the well-known SM results on the two-loop EW contributions to the ρ -parameter. In this case, possible terms proportional to $g^4 m_H^2 m_t^2$ do not appear in the asymptotic limit $m_H \gg m_t$, and the leading terms are only of order $g^4 m_t^2 \log^2(m_H/M_W)$ (see for instance [26]). On this basis, we could conclude that terms proportional to $m_t^2 \Lambda^2$ should not arise at two-loop level, either. Indeed, the Higgs mass appearing in the aforementioned leading terms $\mathcal{O}(g^4 m_t^2 \log^2(m_H/M_W))$ can be interpreted as the effective scale of ChSB for $m_H \gg M_W$. Clearly, a full understanding of this issue in our effective theory needs careful investigations at two-loop level.

4 Higgs boson decay width and branching ratios

We present now numerical results for the Higgs branching ratios and width, for $m_H \lesssim 150$ GeV, as obtained on the basis of the effective Yukawa couplings shown in Table 1. We concentrate

on the Higgs mass range where the Higgs branching ratios show sensitivity to the scale Λ . This occurs for m_H not too close to the threshold for decaying into two real W bosons, where the radiative Yukawa contributions to the Higgs total width become negligible. We will see that, when m_H approaches 150 GeV, the phenomenological features of the effective Yukawa scenario can not be distinguished from the *pure* fermiophobic-Higgs scenario, where all the decays and production channels are computed by assuming that the Higgs boson couples to vector bosons as in the SM, while it has vanishing couplings to all fermions. In all the following tables and figures, the results corresponding to the *pure* fermiophobic-Higgs scenario will be labeled “FP”.

As in the SM, the main Higgs decay channels can be classified into two categories: i) the decays generated at tree-level, $H \rightarrow f\bar{f}$ [27, 28, 29], and $H \rightarrow VV$ [30], with $V = W, Z$, and ii) the loop-induced ones, $H \rightarrow \gamma\gamma$ [29, 31], $H \rightarrow Z\gamma$ [32], and $H \rightarrow gg$ [13, 33]. Since our analysis will be concerned with m_H values below the WW and ZZ kinematical thresholds, the relevant tree-level Higgs decays will be the ones mediated by either on-shell or off-shell EW gauge bosons, namely $H \rightarrow WW^* \rightarrow Wf\bar{f}'$, $H \rightarrow ZZ^* \rightarrow Zf\bar{f}'$, and $H \rightarrow W^*W^* \rightarrow f\bar{f}'f''\bar{f}'''$, $H \rightarrow Z^*Z^* \rightarrow f\bar{f}'f''\bar{f}'''$, where fermions f are summed over all allowed species, and W^* and Z^* are understood to be off shell^{||}.

For Higgs decays into a fermion-pair $H \rightarrow f\bar{f}$, we will use the tree-level SM widths [27, 29], with the SM Yukawa coupling replaced by the effective one evaluated at the m_H scale [cf. eq.(A-1) in the Appendix], thus resumming all the leading logarithmic contributions $g_i^{2n}(\log(\Lambda/m_H))^n$ in the radiative corrections.

The one-loop Higgs decays will all be affected by the suppression of the top Yukawa coupling. The amplitude for the Higgs boson into two gluons ($H \rightarrow gg$) decreases conspicuously (cf. Fig.2), with dramatic consequences on the Higgs production mechanisms at hadron colliders. The leading loop-induced Higgs decays are then $H \rightarrow \gamma\gamma$ and $H \rightarrow Z\gamma$, that receive contribution not only from the top-quark, but also from W loops [29, 31, 32].

In the following, we will always take into account the moderate effect of the radiatively generated top-quark Yukawa coupling in all the one-loop decay channels $H \rightarrow \gamma\gamma$, $H \rightarrow Z\gamma$, and $H \rightarrow gg$, by rescaling the SM top-quark loop amplitude by the ratio $Y_t(m_H)/Y_t^{\text{SM}}$.

Because of the smallness of the effective top-quark Yukawa coupling, neglecting two-loop effects in the $H \rightarrow gg$ decay amplitude will be safe in the present analysis. The analytical form for all Higgs decay widths, used in the following, are reported in the Appendix.

For the SM branching ratios (BR's), we adopted the widths of $H \rightarrow b\bar{b}$ and $H \rightarrow c\bar{c}$ at the (resummed) QCD next to leading order [28], while for Higgs decays into other fermions we kept only the Born approximation with the pole fermion masses [27, 29]. Regarding the SM widths

^{||} From now on, we will label all these final states as WW and ZZ , and omit the $*$ symbol for *off shell* W and Z .

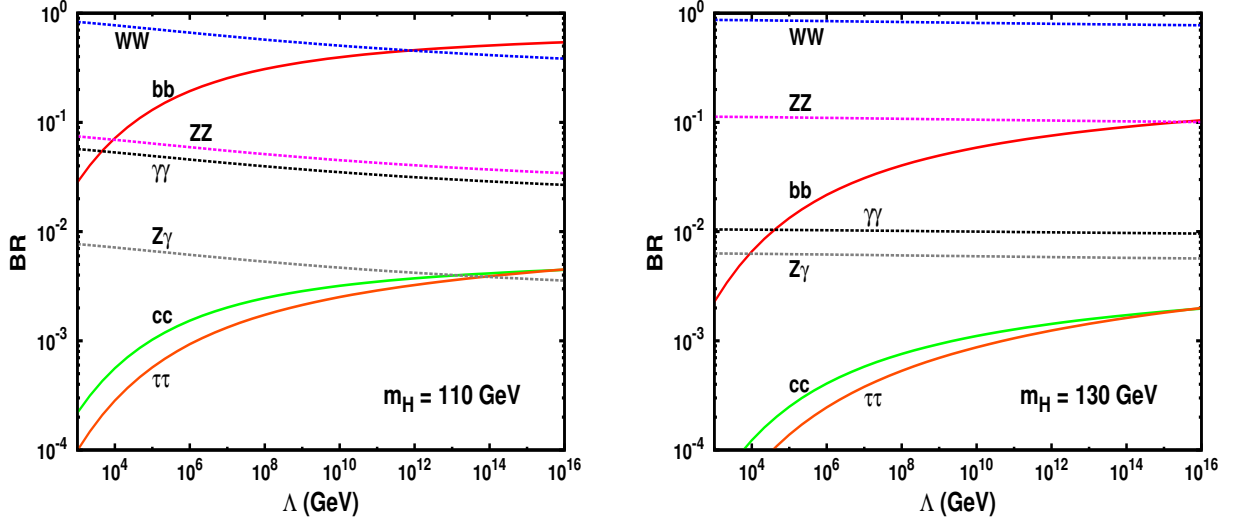


Figure 3: Branching ratios for the Higgs-boson decay into dominant channels, as a function of Λ , for $m_H = 110$ GeV (left), and $m_H = 130$ GeV (right).

of one-loop-induced decays, we neglected higher-order corrections, while for the $H \rightarrow WW$ and $H \rightarrow ZZ$ decays we used the tree-level expression as in eq.(A-2), which includes the 2-, 3-, and 4-bodies decays [34].

In Fig.3, we show the results for Higgs BR's into different final states, for two representative values $m_H = 110$ GeV and $m_H = 130$ GeV, versus the scale Λ , in the range $(10^3 - 10^{16})$ GeV. The numerical values for the same BR's are also reported in table 2, for $\Lambda = 10^{4,6,10,16}$ GeV. From Fig.3 (left), we can see that for $m_H = 110$ GeV the $\text{BR}(b\bar{b})$ can still be conspicuous, and even dominant over the other channels. Its value is about 9.1% for $\Lambda = 10^4$ GeV but can increase up to 40-50%, for $\Lambda > 10^{10}$ GeV. This is a clear effect of the resummation of the leading-log terms, that in $\text{BR}(b\bar{b})$ are particularly large. As a consequence, all the BR's into two gauge bosons are also quite sensitive to the scale Λ , due to the Λ dependence of the Higgs total width.

The $H \rightarrow WW$ channel has a dominant role, too. For $m_H = 110$ GeV, $\text{BR}(WW)$ varies from 78%, at $\Lambda = 10^4$ GeV, down to 38%, at $\Lambda = 10^{16}$ GeV.

Regarding the $H \rightarrow \gamma\gamma$ channel, its BR is about 5.3% for $\Lambda = 10^4$ GeV, and falls down to 2.7%, at $\Lambda = 10^{16}$ GeV (cf. table 2). Although smaller than $\text{BR}(WW)$ and $\text{BR}(b\bar{b})$, the $\text{BR}(\gamma\gamma)$ is strongly enhanced with respect to the SM value [$\text{BR}_{\text{SM}}(\gamma\gamma) = 0.18\%$], when fermion decay modes are radiatively generated.

$\text{BR}(ZZ)$ and $\text{BR}(Z\gamma)$ are also quite sensitive to the scale Λ . They are enhanced with respect to their SM values, and depleted with respect to the fermiophobic-Higgs, for $m_H = 110$ GeV

m_H	Λ	$\gamma\gamma$	WW	ZZ	$Z\gamma$	$b\bar{b}$	$c\bar{c}$	$\tau\bar{\tau}$
(GeV)	(GeV)	BR(%)	BR(%)	BR(%)	BR(%)	BR(%)	BR(%)	BR(%)
100	10^4	12	52	5.1	0.26	30	0.15	0.076
	10^6	8.0	33	3.3	0.17	55	0.28	0.17
	10^{10}	4.6	19	1.9	0.094	74	0.38	0.30
	10^{16}	3.0	12	1.2	0.062	82	0.43	0.44
100	FP	18	74	7.4	0.37	0	0	0
	SM	0.15	1.1	0.11	0.005	82	3.8	8.3
110	10^4	5.3	78	7.0	0.72	9.1	0.071	0.036
	10^6	4.6	66	5.9	0.61	22	0.18	0.11
	10^{10}	3.5	50	4.5	0.46	41	0.33	0.26
	10^{16}	2.7	38	3.4	0.36	54	0.45	0.45
110	FP	5.8	86	7.7	0.79	0	0	0
	SM	0.18	4.6	0.41	0.037	78	3.6	7.9
120	10^4	2.2	85	9.4	0.75	2.6	0.032	0.016
	10^6	2.1	81	8.9	0.72	7.5	0.092	0.056
	10^{10}	1.9	72	8.0	0.64	17	0.21	0.16
	10^{16}	1.7	64	7.1	0.57	26	0.32	0.33
120	FP	2.3	87	9.7	0.77	0	0	0
	SM	0.21	13	1.5	0.11	69	3.2	7.0
130	10^4	1.0	86	11	0.63	0.84	0.016	0.008
	10^6	1.0	85	11	0.62	2.6	0.048	0.029
	10^{10}	1.0	81	11	0.59	6.1	0.12	0.092
	10^{16}	0.96	77	10	0.57	10	0.20	0.20
130	FP	1.0	87	11	0.63	0	0	0
	SM	0.21	29	3.8	0.19	54	2.5	5.4
140	10^4	0.53	87	12	0.48	0.29	0.008	0.004
	10^6	0.53	86	12	0.48	0.90	0.026	0.016
	10^{10}	0.53	85	12	0.47	2.3	0.064	0.051
	10^{16}	0.52	83	11	0.46	4.1	0.11	0.12
140	FP	0.53	87	12	0.48	0	0	0
	SM	0.19	48	6.6	0.24	36	1.6	3.6

Table 2: Branching ratios (in percentage) for dominant Higgs boson decay channels, at different values of the Higgs mass and Λ . The SM and FP rows present the SM and fermiophobic-Higgs scenario results, respectively.

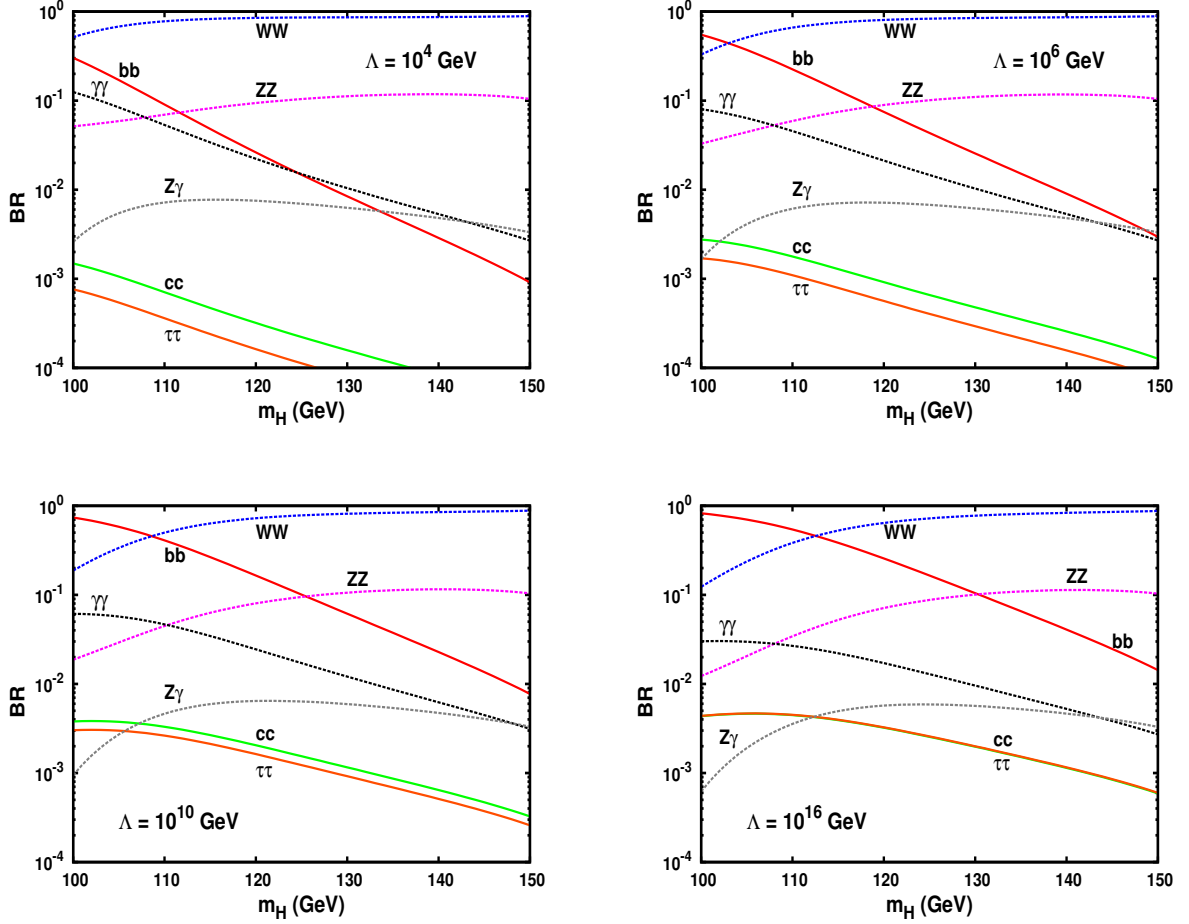


Figure 4: Higgs branching ratios for different decay channels versus the Higgs mass, for four representative values $\Lambda = 10^{4,6,10,16}$ GeV.

(cf. table 2). Note that $\text{BR}(c\bar{c})$ and $\text{BR}(\tau\bar{\tau})$ become comparable to $\text{BR}(Z\gamma)$ when $\Lambda > 10^{10}$ GeV, for $m_H = 110$ GeV.

At $m_H = 100$ GeV, the enhancement of all the fermionic decays is even more dramatic (cf. table 2). On the other hand, when $m_H > 110$ GeV, the BR hierarchy for the different decay channels gets modified [see Fig.3 (right)]. The fermionic decays get depleted, while both $\text{BR}(WW)$ and $\text{BR}(ZZ)$ increase, and lose sensitivity to Λ , due to the fast grow of the $H \rightarrow WW$ and $H \rightarrow ZZ$ decay widths when approaching the real WW threshold. The rates for one-loop decays ($H \rightarrow \gamma\gamma$, particularly) also get smaller.

At $m_H \simeq 150$ GeV, one can hardly distinguish the effective Yukawa's scenario from the pure fermiophobic-Higgs one, if not at very large Λ . One can reach $\text{BR}(\bar{b}b) \gtrsim 0.3\%$ for $\Lambda \gtrsim 10^6$ GeV, and $\text{BR}(\bar{b}b) \gtrsim 1.4\%$ for $\Lambda \gtrsim 10^{16}$ GeV. This can be checked in Fig.4, where we show the main

$\Lambda(\text{GeV})$	$\Gamma_H^{100}(\text{MeV})$	$\Gamma_H^{110}(\text{MeV})$	$\Gamma_H^{120}(\text{MeV})$	$\Gamma_H^{130}(\text{MeV})$	$\Gamma_H^{140}(\text{MeV})$
10^4	5.3×10^{-2}	1.7×10^{-1}	5.8×10^{-1}	1.7	4.6
10^6	8.3×10^{-2}	2.0×10^{-1}	6.1×10^{-1}	1.7	4.7
10^{10}	1.5×10^{-1}	2.7×10^{-1}	6.8×10^{-1}	1.8	4.7
10^{16}	2.2×10^{-1}	3.5×10^{-1}	7.6×10^{-1}	1.9	4.8
FP	3.7×10^{-2}	1.6×10^{-1}	5.6×10^{-1}	1.7	4.6
SM	2.6	3.0	3.7	5.1	8.3

Table 3: Total width $\Gamma_H^{m_H}$ of the Higgs boson for different m_H (expressed in GeV) and Λ . The last two rows show the fermiophobic-Higgs (FP) and SM cases, respectively.

Higgs BR's versus the Higgs mass, for $\Lambda = 10^{4,6,10,16}$ GeV. While the tree-level Higgs BR's in EW gauge bosons become almost insensitive to the scale Λ for Higgs masses larger than 130 GeV, the Higgs rates for decays into $b\bar{b}$, $c\bar{c}$, and $\tau\bar{\tau}$, although depleted at $m_H \sim 150$, keep their sensitivity to Λ in all the m_H range considered**.

In table 3, we show the results for the Higgs total width $\Gamma_H^{m_H}$ for different values of the Higgs mass and Λ . For comparison, the corresponding FP and SM values are shown in the last two rows of the same table. At $m_H = 110$ GeV, a considerable depletion of the total width is seen with respect to the SM one ($\Gamma_{\text{SM}} = 3.0$ MeV). The corresponding Γ_H ranges from $\Gamma_H = 0.17$ MeV for $\Lambda = 10^4$ GeV up to $\Gamma_H = 0.35$ MeV for $\Lambda = 10^{16}$ GeV. This is mainly due to the $\Gamma(H \rightarrow b\bar{b})$ suppression by Yukawa effective couplings. For larger m_H , the total width substantially approaches the SM value (and matches the FB value), since the tree-level decays $H \rightarrow WW, ZZ$ become dominant near the WW threshold.

In Fig.5, the Higgs BR's, normalized to the corresponding SM values, are shown. Although all the Higgs decays in EW gauge bosons are enhanced with respect to the SM, the most substantial effect is observed in the $H \rightarrow \gamma\gamma$ channel. For instance, $\text{BR}(\gamma\gamma)$, at $m_H = 110$ GeV and for $\Lambda = 10^{4(16)}$ GeV, is enhanced up to 29 (14) times the SM value, while for $\text{BR}(WW)$, $\text{BR}(ZZ)$, and $\text{BR}(Z\gamma)$ the enhancement factor is about 19 (9.5). As for the Λ dependence, at large Λ the decay widths into fermion pairs tend to be wider, and the enhancement of the decays into EW gauge bosons drops.

The larger enhancement for $\text{BR}(\gamma\gamma)$ with respect to the $\text{BR}(WW)$ and $\text{BR}(ZZ)$ cases is due to the destructive interference, in the SM, between the top-quark loop and the W loop in $H \rightarrow \gamma\gamma$, that is suppressed in the present scenario. The same holds for the smaller enhancement in the $H \rightarrow Z\gamma$ BR, that is however less affected by the top-quark loop.

** $\text{BR}(\mu\mu)$, that is of order $\mathcal{O}(10^{-5})$, is also very sensitive to the scale Λ .

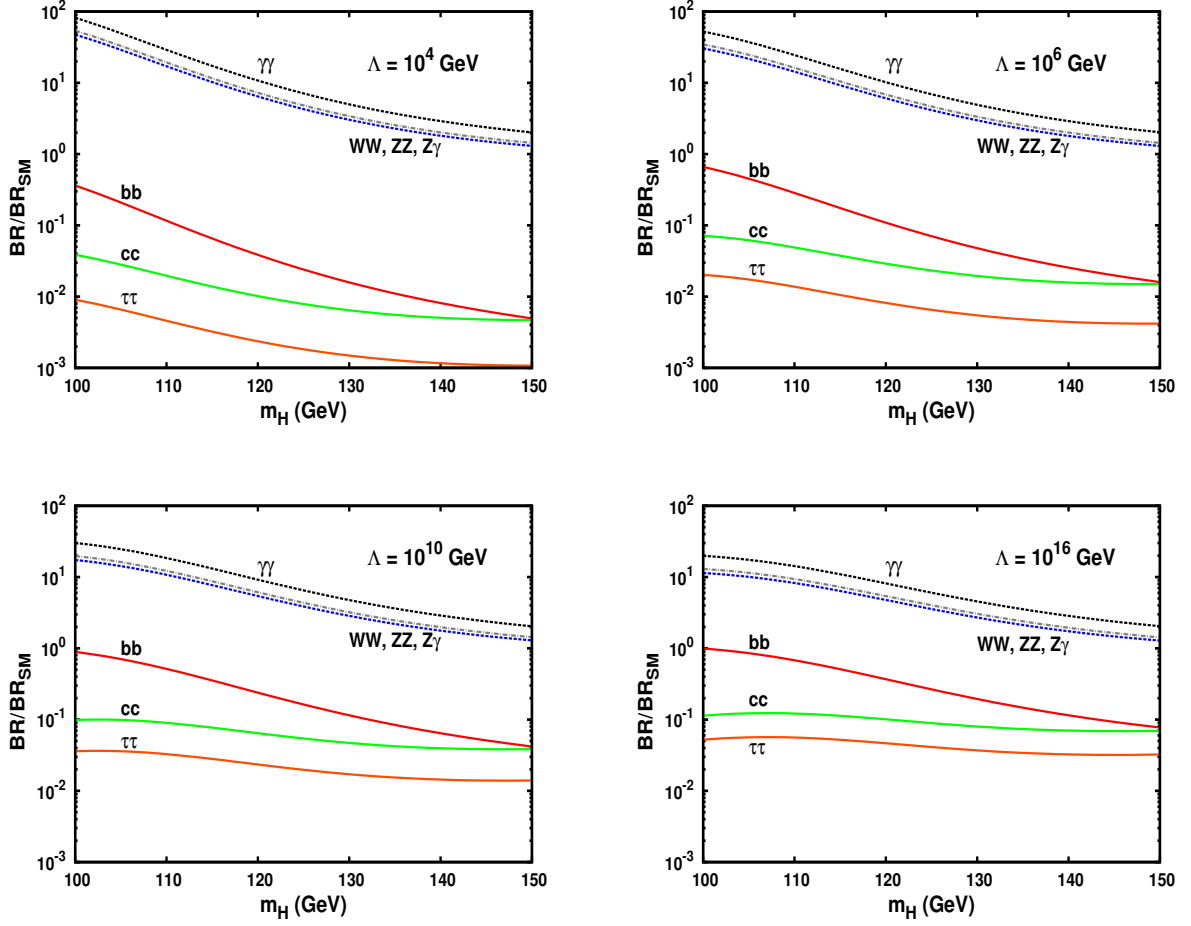


Figure 5: Higgs branching ratios normalized to the SM values, for the dominant decay channels, versus m_H , and for a few representative values of Λ . Note that the $Z\gamma$ curves are the upper ones among the almost degenerate WW , ZZ , and $Z\gamma$ sets.

5 Production cross sections for different Higgs boson signatures

In this section, we will present Higgs production cross sections at hadron colliders, corresponding to different Higgs decay channels, in the effective Yukawa scenario.

Experimental strategies to constrain this scenario can be elaborated on the basis of existing LEP and Tevatron data. As already mentioned, the most stringent bounds on m_H in the *pure* fermiophobic Higgs scenario have been obtained at LEP ($m_H > 109.7$ GeV at 95% C.L. [15]) by studying the process $e^+e^- \rightarrow HZ$, with $H \rightarrow \gamma\gamma$, and at the Tevatron ($m_H > 106$ GeV at 95% C.L., corresponding to 3.0 fb^{-1} of analyzed data [16, 17]), via both Higgsstrahlung $p\bar{p} \rightarrow HV \rightarrow \gamma\gamma + X$, and VBF $p\bar{p} \rightarrow VV + X \rightarrow H + X \rightarrow \gamma\gamma + X$. Effective Yukawa couplings deplete $\text{BR}(H \rightarrow \gamma\gamma)$ with respect to the fermiophobic-Higgs scenario, due to the nonvanishing $\Gamma(H \rightarrow \bar{f}f)$ contribution to the total width (cf. table 2). Then, we expect the analysis in [15, 16, 17], when applied to our model, should end up into weaker bounds on the Higgs mass, depending on the scale Λ . Note, however, that the fermionic decays would play an extra role in excluding m_H ranges at LEP, with respect to a *pure* fermiophobic Higgs scenario. In the following, we will present our results for $m_H \geq 100$ GeV, that, we expect on the basis of the results in table 2, should cover all the experimentally allowed region.

The Tevatron has a considerable potential for constraining models with enhanced $\text{BR}(H \rightarrow \gamma\gamma)$ [35]. Present searches are sensitive, in the range $115 \text{ GeV} \leq m_H \leq 130 \text{ GeV}$, to scenarios where the $H \rightarrow \gamma\gamma$ rate is enhanced by at least a factor of about 20 with respect to its SM value [16]. With 2.7 fb^{-1} of integrated luminosity, a 95% C.L. upper limit on $\text{BR}(H \rightarrow \gamma\gamma)$ between 14.1% and 33.9%, for $100 \text{ GeV} \leq m_H \leq 150 \text{ GeV}$, has been derived by D0, for models where the Higgs does not couple to the top quark. This is not yet sufficient to test the effective Yukawa coupling scenario, that, for $\Lambda \gtrsim 10^4$ GeV, predicts $\text{BR}(H \rightarrow \gamma\gamma) \lesssim 12\%$ in this m_H range (cf. table 2).

In Fig.6, we present the total cross sections times the Higgs branching ratios for different decay channels, in $p\bar{p}$ collisions at Tevatron, with c.m energy $\sqrt{S} = 1.96$ TeV. In particular, we consider the Higgs decay channels $H \rightarrow \gamma\gamma, b\bar{b}, WW, ZZ$. Solid (red) lines correspond to the inclusive cross section for VBF + HW + HZ production (labeled VB in the figure) in the effective Yukawas model, for $\Lambda = 10^{4,6,10,16}$ GeV. The dashed (blue) lines and dot-dashed (grey) lines correspond to the SM (mediated by either gg fusion or VB), and fermiophobic-Higgs (FP) scenario (with vanishing Yukawa couplings), respectively. We did not include, in the effective Yukawa model predictions, the gluon fusion contribution, that is expected to be suppressed by more than a factor 10^{-2} with respect to the SM cross section (cf. Y_t values in table 1). Cross sections are computed at NLO, and presented by their central values, neglecting different

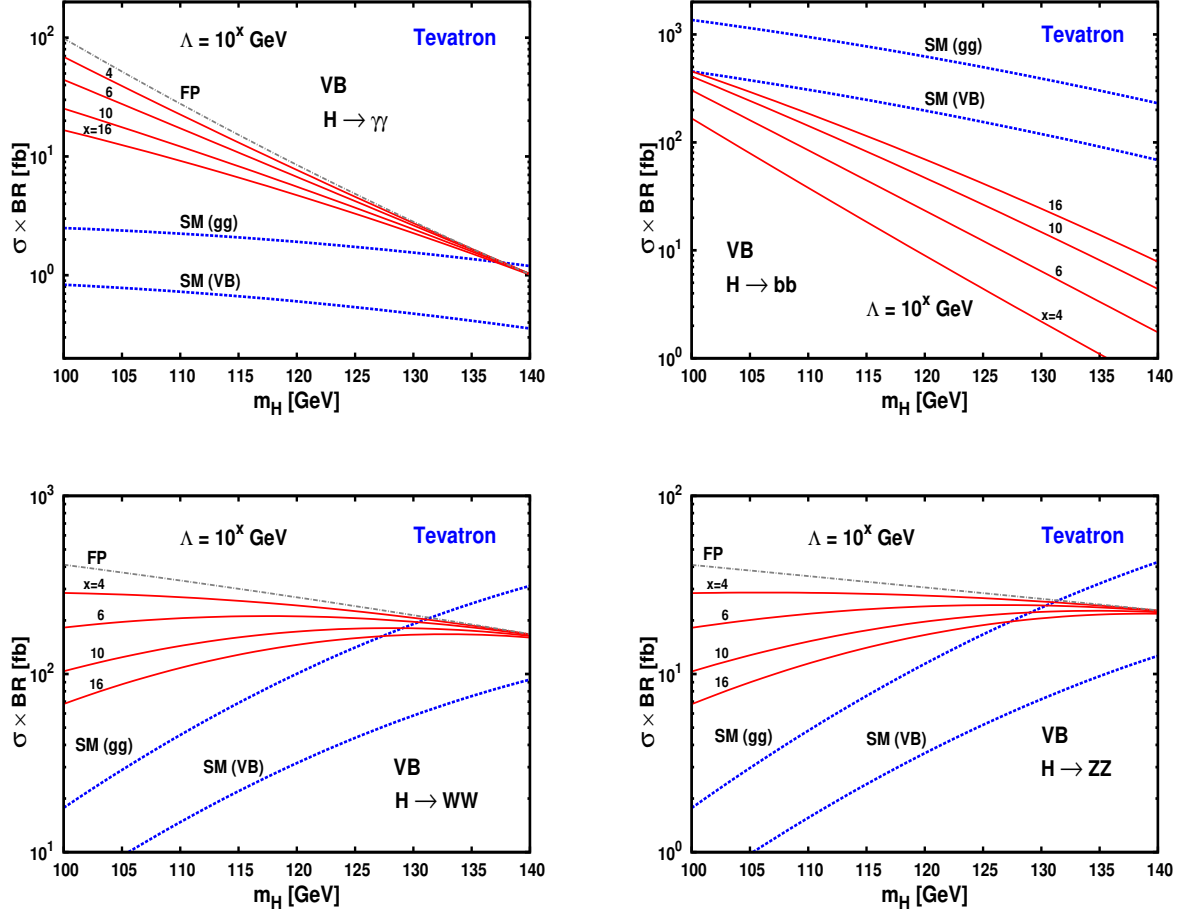


Figure 6: Total cross sections times Higgs branching ratios for $p\bar{p}$ collisions at Tevatron, with c.m. energy $\sqrt{S} = 1.96$ TeV, for the Higgs decays $H \rightarrow \gamma\gamma$, $b\bar{b}$, WW , ZZ , versus the Higgs mass. Continuous (red) lines correspond to the VB predictions in the effective Yukawas model, for $\Lambda = 10^{4,6,10,16}$ GeV, with VB standing for the inclusive cross section for VBF + HW + HZ . The dashed (blue) lines and dot-dashed (grey) lines correspond to the SM (mediated by either gg fusion or VB processes) and fermiophobic Higgs scenario (FP), respectively.

Λ (GeV)	R_σ^{100}	R_σ^{120}	R_σ^{140}
10^4	2.1×10^{-3}	3.5×10^{-3}	5.5×10^{-3}
10^6	6.0×10^{-3}	1.1×10^{-2}	1.7×10^{-2}
10^{10}	1.5×10^{-2}	2.6×10^{-2}	4.4×10^{-2}
10^{16}	2.5×10^{-2}	4.7×10^{-2}	7.9×10^{-2}

Table 4: Ratio $R_\sigma^{m_H} = \tilde{\sigma}_{gg}/\sigma_{\text{VBF}}$ of total cross sections for Higgs production via gluon fusion and via VBF in the effective Yukawa model at the LHC, with $\sqrt{S} = 14$ TeV, for representative values of Λ and m_H , expressed in GeV.

theoretical uncertainties, as obtained from [36].

While the $H \rightarrow b\bar{b}$ channel tends to be considerably more difficult than in the SM, there is a remarkable enhancement, not only in the $H \rightarrow \gamma\gamma$ decay, but also in the $H \rightarrow WW, ZZ$ channels, for masses up to $m_H \sim 125$ GeV. For lower Higgs masses, the sensitivity to the scale Λ is quite large.

Expectations for cross sections times branching ratios at the LHC are presented in Figs.7 and 8, for the c.m. energy $\sqrt{S} = 14$ TeV. In particular, Fig.7 refers to the one-loop decays $H \rightarrow \gamma\gamma$ (top), and $H \rightarrow Z\gamma$ (bottom), while Fig.8 refers to the tree-level decays $H \rightarrow WW$ (top), and $H \rightarrow ZZ$ (bottom). In general, conventions in Figs.7 and 8 are the same as for the Tevatron case in Fig.6, but for the LHC we show only the production via VBF, and discuss the associated HW and HZ production later on. Cross sections are computed as for Fig.6^{††}.

At the LHC the SM gluon fusion production plays a more relevant role than at the Tevatron. It is then interesting to have a look at the depleted gg contribution to the total cross section arising in the effective Yukawa scenario. In table 4, we present the ratio $R_\sigma^{m_H} = \tilde{\sigma}_{gg}/\sigma_{\text{VBF}}$ of total cross sections for Higgs production via gluon fusion ($\tilde{\sigma}_{gg}$) and via VBF (σ_{VBF}) [36], in the effective Yukawa model, at the LHC with $\sqrt{S} = 14$ TeV. We present results for $\Lambda = 10^{4,6,10,16}$ GeV, and $m_H = 100, 120, 140$ GeV.

The gluon fusion cross section $\tilde{\sigma}_{gg}$ has been computed by rescaling the SM values at NNLL+NNLO [37] by the factor due to the top-quark Yukawa suppression $(Y_t(m_H)/Y_t^{\text{SM}})^2$. One can see that the gluon fusion cross section is at most a few percent of the VBF cross section, in the range of m_H and Λ considered. We will neglect here this contribution.

As one can see from Figs.7 and 8, at the LHC the depletion in the total cross section with respect to the SM gluon fusion mechanism is, for $m_H \lesssim 130$ GeV, largely compensated for by

^{††}The SM gluon fusion cross sections at the (resummed) NNLL+NNLO have been obtained by the online calculator by M. Grazzini, for the parton distribution functions set MSTW2008 NNLO [37].

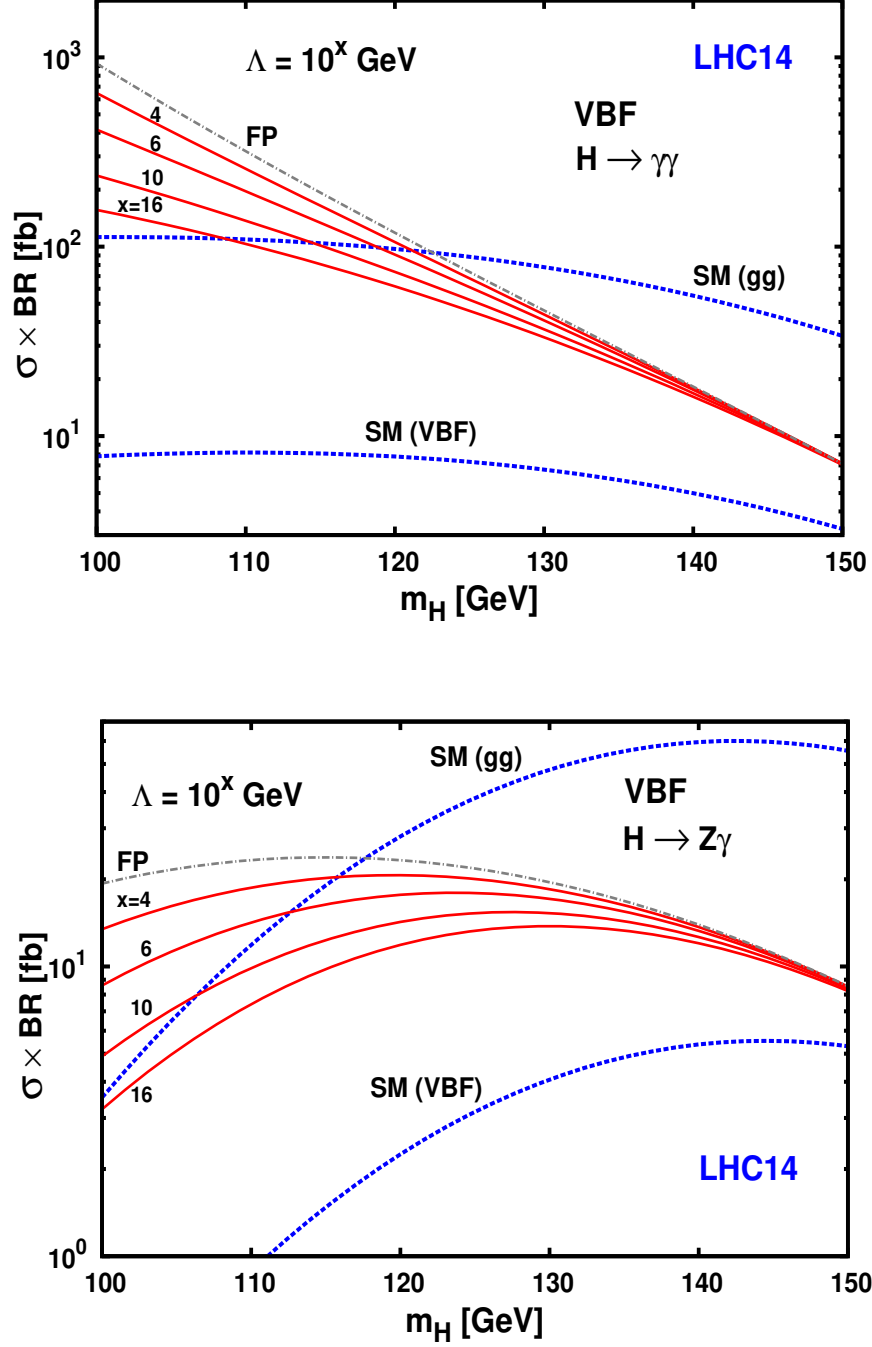


Figure 7: Total cross sections times Higgs branching ratios, for pp collisions at the LHC with c.m. energy $\sqrt{s} = 14$ TeV, for the Higgs decaying into the loop-induced modes $H \rightarrow \gamma\gamma$ (top) and $H \rightarrow Z\gamma$ (bottom), versus the Higgs mass. Continuous (red) lines correspond to the VBF predictions in the effective Yukawas model, for $\Lambda = 10^{4,6,10,16}$ GeV. The dashed (blue) lines and dot-dashed (grey) lines correspond to the SM (mediated by either gg fusion or VBF) and fermiophobic Higgs scenario (FP), respectively.

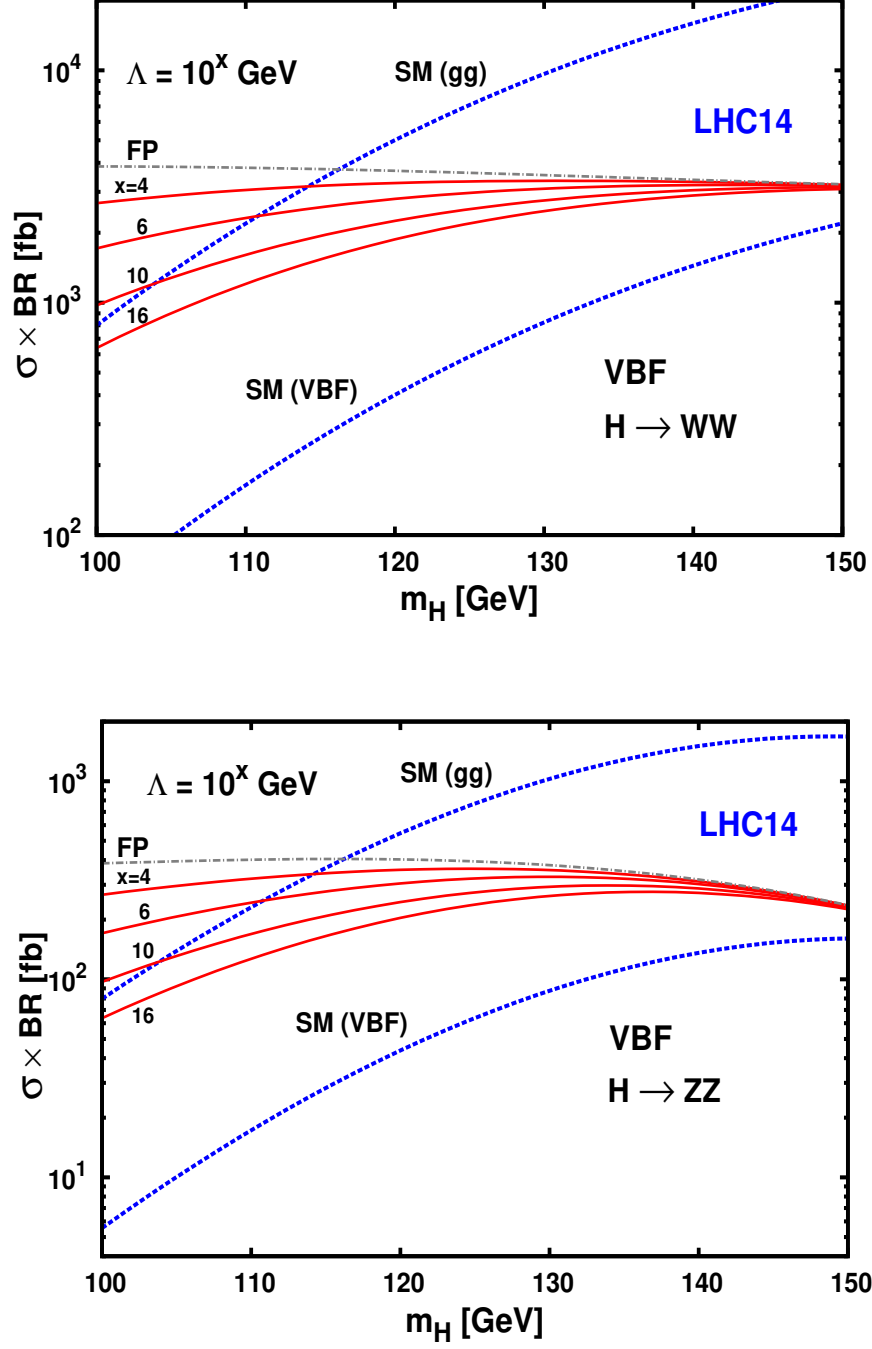


Figure 8: Total cross sections times Higgs branching ratios, for pp collisions at the LHC with c.m. energy $\sqrt{s} = 14$ TeV, for the Higgs decaying into tree-level modes $H \rightarrow WW$ (top) and $H \rightarrow ZZ$ (bottom), versus the Higgs mass. Continuous (red) lines correspond to the VBF predictions in the effective Yukawas model, for $\Lambda = 10^4, 6, 10, 16$ GeV. The dashed (blue) lines and dot-dashed (grey) lines correspond to the SM (mediated by either gg fusion or VBF) and fermiophobic-Higgs scenario (FP), respectively.

the enhancements in the BR's. The sensitivity to the scale Λ is considerable, in this m_H range. Notice that, while the $H \rightarrow \gamma\gamma$ cross section falls by more than 1 order of magnitude when m_H moves from 100 GeV to 150 GeV, for the $H \rightarrow WW, ZZ, Z\gamma$ channels the VBF cross section drop at larger m_H is more than compensated for by the rise in the corresponding BR's (cf. fig.4).

The combined analysis of the $H \rightarrow \gamma\gamma, Z\gamma, WW, ZZ$ channels, at integrated luminosities of a few 10 fb^{-1} , could clearly distinguish an anomalous VBF signal corresponding to effective Yukawa couplings, that should replace the dominant gluon fusion signature in the SM cross sections.

The enhanced $\text{BR}(H \rightarrow \gamma\gamma)$ also makes the WH/ZH associated production with $H \rightarrow \gamma\gamma$ at the LHC a remarkably promising channel, that could be studied for inclusive W/Z decays. Total cross sections times Higgs branching ratios are shown in the upper part of Fig.9, for pp collisions at c.m. energy $\sqrt{S} = 14 \text{ TeV}$, for the associated HW (left) and HZ (right) Higgs production, with $H \rightarrow \gamma\gamma$. WH/ZH production rates are according to [36]. The enhancement for the $\gamma\gamma$ signature with respect to the SM scenario, and the easy topology of the WH/ZH events could make the Higgs associated production a crucial handle in the experimental establishment of the effective Yukawa scenario at the LHC.

On the other hand, it could be harder at the LHC pinpointing the depleted fermionic Higgs decays like $H \rightarrow b\bar{b}$ and $\tau\tau$, the first also being challenging in the *easier* SM scenario, the latter being very much suppressed in the radiative Yukawa framework (cf. Fig. 5). However, in view of the new techniques for b -jet tagging in Higgs associated production that are being developed at the LHC [38], we also plot in the lower part of Fig.9 the corresponding $H \rightarrow b\bar{b}$ cross sections for the HW (left) and HZ (right) associated production. Further advances in the b -jets tagging technique seem to be required to gain some sensitivity to the $H \rightarrow b\bar{b}$ rates predicted in our model.

In Fig.10, the total cross sections times the Higgs branching ratios are presented for LHC collisions at $\sqrt{S} = 7 \text{ TeV}$. Four cases, corresponding to the Higgs decays into EW gauge bosons $H \rightarrow \gamma\gamma, Z\gamma, WW, ZZ$, are shown, as in the previous $\sqrt{S} = 14 \text{ TeV}$ case.

Here, we also neglect the top-loop gluon fusion production, that, on the other hand, due to the enhanced SM ratio σ_{gg}/σ_{VBF} at 7 TeV with respect to the 14 TeV case, can lead to an almost sizable contribution to the total cross section^{‡‡}.

Nevertheless, VBF total cross section for effective Yukawa couplings is in this case quite moderate. In particular, it drops by more than 1 order of magnitude, for \sqrt{S} falling from 14 TeV down to 7 TeV. Any study directed to pinpoint an anomalous behavior of the Higgs Yukawa

^{‡‡}In Fig.10, total cross sections corresponding to the SM gluon-fusion and VBF productions are at NNLL+NNLO [37] and at NNLO [12], respectively.

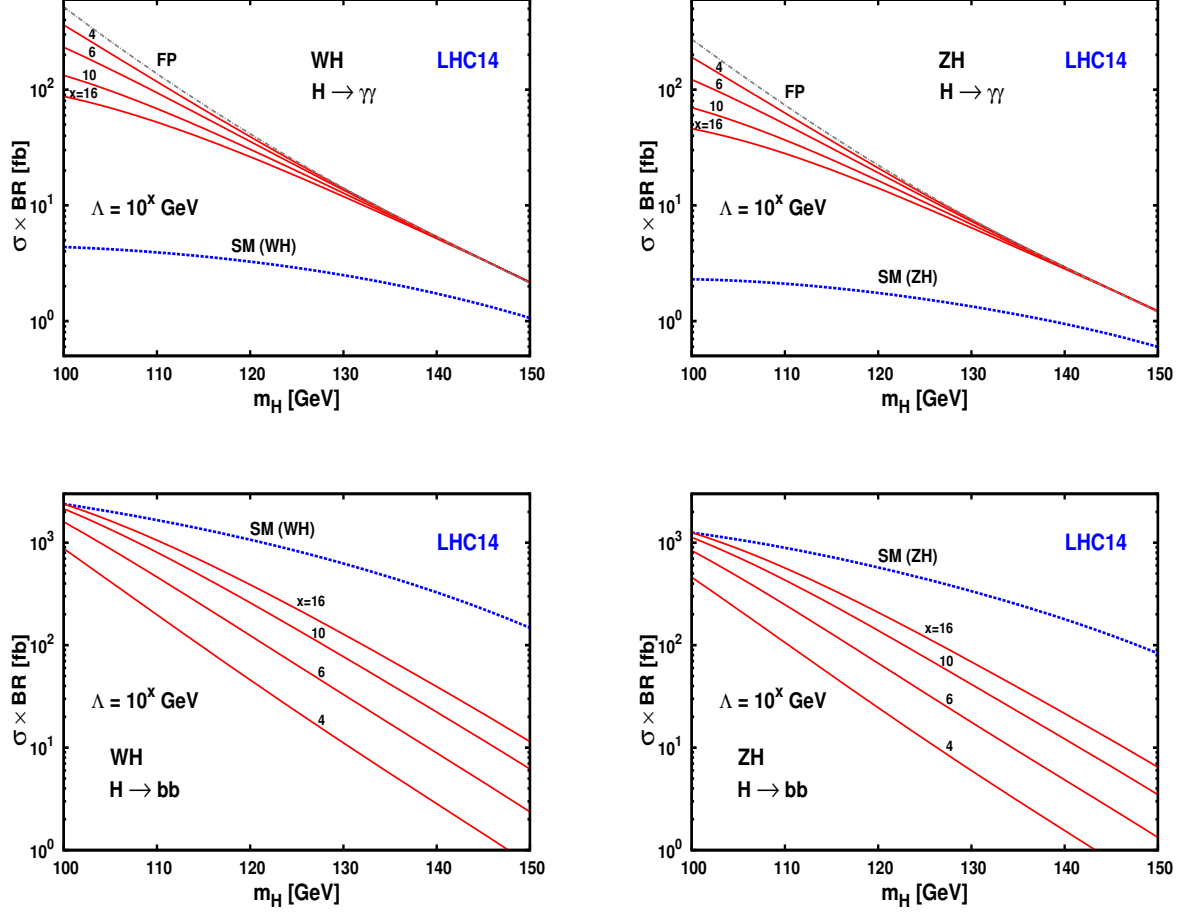


Figure 9: Total cross sections times Higgs branching ratios, for pp collisions at the LHC with c.m. energy $\sqrt{S} = 14$ TeV, via the WH (left) and ZH (right) associated Higgs production mechanism, for the Higgs decaying into $\gamma\gamma$ (top) and $b\bar{b}$ (bottom) modes, versus the Higgs mass. Continuous (red) lines correspond to the predictions in the effective Yukawas model, for $\Lambda = 10^{4,6,10,16}$ GeV. The dashed (blue) lines and dot-dashed (grey) lines correspond to the SM and fermiophobic Higgs scenario (FP), respectively.

couplings seems to be out of reach, for the limited amount of integrated luminosity (i.e., a few fb's) that is presently foreseen for the 7 TeV run of the LHC.

6 Conclusions

In this paper, we studied the phenomenological consequences of a theoretical framework where a Higgs boson gives masses to EW gauge bosons as in the SM, but it is not responsible for the generation of fermion masses. By setting the Higgs Yukawa couplings to zero at a scale Λ (connected to the new mechanism for fermion mass generation), nonvanishing Yukawa couplings arise radiatively, as an effect of chiral symmetry breaking by explicit fermion mass terms. We computed these effects by RG equation techniques. A nontrivial pattern for Higgs BR's in different channels ensues in the range $100 \text{ GeV} \lesssim m_H \lesssim 150 \text{ GeV}$, with enhanced $H \rightarrow \gamma\gamma$, WW , ZZ , $Z\gamma$ decays, and non negligible decay rates into heavy-fermion pairs. VBF replaces gluon fusion as the main Higgs boson production channel at the LHC, with quite considerable sensitivity to the Λ scale in different decay signatures, for $m_H \lesssim (130 - 140) \text{ GeV}$.

Present data from LEP [15] and the Tevatron [16, 17] can constrain this scenario today . A dedicated analysis is needed, combining the effects of the simultaneous enhancement of the $H \rightarrow \gamma\gamma$ decay and the nontrivial depletion of the $H \rightarrow b\bar{b}$ decay, in order to find m_H bounds versus Λ (that, we stress, is the only new free parameter of the model). The final potential of the Tevatron will depend on the integrated luminosity collected. However, on the basis of present analysis carried out for the fermiophobic Higgs scenario [16, 17], it seems unlikely that Tevatron can probe the effective Yukawa scenario in the mass range $m_H \gtrsim 110 \text{ GeV}$, with an integrated luminosity of about 10 fb^{-1} .

The potential of the LHC at $\sqrt{S} = 14 \text{ TeV}$ in further probing the effective Yukawa scenario looks excellent, deserving an accurate and dedicated analysis. On the one hand, the enhanced VBF production for different Higgs signatures gives rise to total cross sections that are in general larger than, or comparable with, the SM ones for $m_H \lesssim 120 \text{ GeV}$, and will benefit, even for larger m_H , from the better signal-to-background ratio that VBF production enjoys with respect to the gluon fusion mechanism. On the other hand, the excellent theoretical accuracy in the prediction of VBF processes [12] could help to probe the cross section sensitivity to the scale Λ , even beyond $m_H \sim 130 \text{ GeV}$. Furthermore, a remarkably promising role will be also played by the inclusive WH/ZH associated production, when $H \rightarrow \gamma\gamma$.

Much better performances in precision measurements of the Higgs couplings are expected of course from a possible e^+e^- collider program [39]. That could eventually also allow a quite accurate Λ determination for $m_H > 130 \text{ GeV}$ and to directly test the radiatively induced Yukawa couplings.

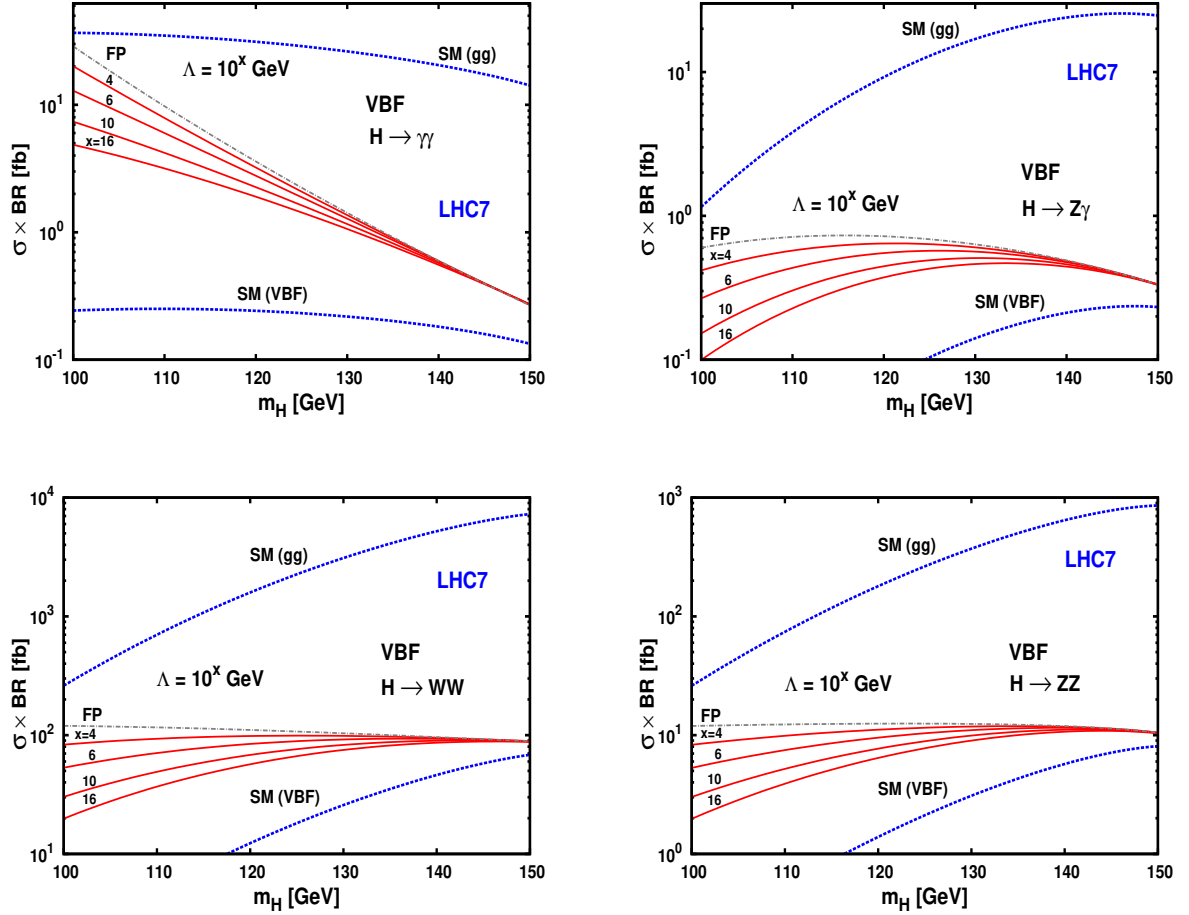


Figure 10: Total cross sections times Higgs branching ratios, for pp collisions at the LHC with c.m. energy $\sqrt{S} = 7$ TeV, for the Higgs decaying into EW gauge bosons $H \rightarrow \gamma\gamma$, $Z\gamma$, WW , ZZ , versus the Higgs mass. Continuous (red) lines correspond to the VBF predictions in the effective Yukawas model, for $\Lambda = 10^{4,6,10,16}$ GeV. The dashed (blue) lines and dot-dashed (grey) lines correspond to the SM (mediated by either gg fusion or VBF) and fermiophobic Higgs scenario (FP), respectively.

Acknowledgments

We would like to thank Gian Giudice for many enlightening discussions. We also benefitted from conversations with Giuseppe Degrandi, Gino Isidori, Mauro Moretti, Fulvio Piccinini, and Alessandro Strumia. We thank Fabio Maltoni and Marco Zaro for providing us LHC Higgs production cross sections at $\sqrt{S} = 7$ TeV. B.M. was partially supported by the RTN European Programme Contract No. MRTN-CT-2006-035505 (HEPTOOLS, Tools and Precision Calculations for Physics Discoveries at Colliders).

Appendix

We provide here the main formula used for the calculation of the partial widths in the present model. The decays of the Higgs boson with mass $m_H < 150$ GeV can be classified as tree-level and loop-induced channels. The corresponding decay widths are given by

- **Tree-level** [27, 29, 30, 34]

$$\Gamma(H \rightarrow f\bar{f}) = \frac{N_c m_H |Y_f(m_H)|^2}{16\pi} \left(1 - 4\frac{m_f^2}{m_H^2}\right)^{3/2} \quad (\text{A-1})$$

$$\Gamma(H \rightarrow V^*V^*) = \frac{1}{\pi^2} \int_0^{m_H^2} \frac{d\mu_1^2 M_V \Gamma_V}{(\mu_1^2 - M_V^2)^2 + M_V^2 \Gamma_V^2} \int_0^{(m_H - \mu_1)^2} \frac{d\mu_2^2 M_V \Gamma_V}{(\mu_2^2 - M_V^2)^2 + M_V^2 \Gamma_V^2} \Gamma_0 \quad (\text{A-2})$$

where $Y_f(m_H)$ is the effective Yukawa coupling of the fermion f evaluated at the scale m_H , $x_i = m_i^2/m_H^2$, and the squared matrix element Γ_0 for the decay $H \rightarrow V^*V^*$, is given by

$$\Gamma_0 = \frac{G_F m_H^3}{16\sqrt{2}\pi} \delta_V \sqrt{\lambda(\mu_1^2, \mu_2^2, m_H^2)} \left(\lambda(\mu_1^2, \mu_2^2, m_H^2) + \frac{12\mu_1^2 \mu_2^2}{m_H^4} \right) \quad (\text{A-3})$$

with $\lambda(x, y, z) = (1 - x/z - y/z)^2 - 4xy/z^2$ and $\delta_V = 2(1)$ for $V = W(Z)$. Equation (A-2) includes the 2-, 3-, and 4-bodies decays.

- **One-loop-induced** [13, 29, 31, 32, 33]

$$\Gamma(H \rightarrow \gamma\gamma) = \frac{G_F \alpha^2 m_H^3}{128\sqrt{2}\pi^3} \left| \frac{4}{9} N_c A_t(y_t) \xi_t + A_W(y_W) \right|^2 \quad (\text{A-4})$$

$$\Gamma(H \rightarrow gg) = \frac{G_F \alpha_s^2 m_H^3}{36\sqrt{2}\pi^3} \left| \frac{3}{4} A_t(y_t) \xi_t \right|^2 \quad (\text{A-5})$$

$$\Gamma(H \rightarrow Z\gamma) = \frac{G_F^2 M_W^2 \alpha m_H^3}{64\pi^4} \left(1 - \frac{M_Z^2}{m_H^2}\right)^3 |B_t(\tau_t, \lambda_t) \xi_t + c_W B_W(\tau_W, \lambda_W)|^2 \quad (\text{A-6})$$

$G_F(\text{GeV}^{-2})$	$M_W(\text{GeV})$	$M_Z(\text{GeV})$	$\Gamma_W(\text{GeV})$	$\Gamma_Z(\text{GeV})$	$m_t(\text{GeV})$	$m_b(\text{GeV})$
$1.16637 \cdot 10^{-5}$	80.398	91.1875	2.141	2.4952	171.3	4.88
$m_c(\text{GeV})$	$m_s(\text{MeV})$	$m_\tau(\text{GeV})$	$m_\mu(\text{MeV})$	$\alpha^{-1}(M_Z)$	$\alpha^{-1}(0)$	$\alpha_S(M_Z)$
1.64	105	1.77684	105.658	128.9	137.036	0.1172

Table 5: Values for the SM input parameters used for the numerical results. The quark masses correspond to their pole masses.

where $y_t = m_H^2/(4m_t^2)$, $y_W = m_H^2/(4M_W^2)$, $\tau_i = 1/y_i$, $\lambda_t = 4m_t^2/M_Z^2$, $\lambda_W = 4M_W^2/M_Z^2$, and

$$\begin{aligned}
A_W(x) &= -\frac{2x^2 + 3x + 3(2x-1)F(x)}{x^2} \\
A_t(x) &= \frac{2(x + (x-1)F(x))}{x^2} \\
B_t(x, y) &= \frac{2N_c}{3c_W} \left(1 - \frac{8}{3}s_W^2\right) (I_1(x, y) - I_2(x, y)) \\
B_W(x, y) &= 4 \left(3 - \frac{s_W^2}{c_W^2}\right) I_2(x, y) + \left[\left(1 + \frac{2}{x}\right) \frac{s_W^2}{c_W^2} - \left(5 + \frac{2}{x}\right) \right] I_1(x, y), \quad (\text{A-7})
\end{aligned}$$

where $c_W = \cos \theta_W$ and $s_W = \sin \theta_W$, with θ_W the Weinberg angle. The functions $I_{1,2}(x, y)$ are given by

$$\begin{aligned}
I_1(x, y) &= \frac{xy}{2(x-y)} + \frac{x^2y^2}{2(x-y)^2} (F(\bar{x}) - F(\bar{y})) + \frac{x^2y}{(x-y)^2} (G(\bar{x}) - G(\bar{y})) \\
I_2(x, y) &= -\frac{xy}{2(x-y)} (F(\bar{x}) - F(\bar{y})) \quad (\text{A-8})
\end{aligned}$$

with $F(x) = (\arcsin \sqrt{x})^2$, $G(x) = \sqrt{\frac{1-x}{x}} \arcsin \sqrt{x}$, and $\bar{x} = 1/x$, $\bar{y} = 1/y$. In eqs.(A-4)-(A-6), $\xi_f = 1$ and $\xi_t = Y_t(m_H)/Y_t^{\text{SM}}$ for the SM and effective Yukawa model, respectively, with $Y_t(m_H)$ evaluated at the scale m_H . The electromagnetic coupling constant α , appearing in eqs. (A-4) and (A-6), is taken at the scale $q^2 = 0$, namely $\alpha(0)$, since the final state photons in the Higgs decays $H \rightarrow \gamma\gamma$ and $H \rightarrow Z\gamma$ are on shell. For the strong coupling α_S appearing in eq.(A-5), we assume $\alpha_S = \alpha_S(M_Z)$.

All the SM input parameters in the numerical analysis are given in table 5 [40].

References

- [1] S. L. Glashow, Nucl. Phys. **22** (1961) 579; S. Weinberg, Phys. Rev. Lett. **19** (1967) 1264. A. Salam, in *Elementary Particle Theory*, Nobel Symposium No.8, ed. N. Svartholm, pp. 367 (Almqvist and Wiksell, Stockholm, 1968).
- [2] C. Quigg, Ann. Rev. Nucl. Part. Sci. **59** (2009) 505 [arXiv:0905.3187 [hep-ph]].
- [3] A. Djouadi, Phys. Rept. **457** (2008) 1 [arXiv:hep-ph/0503172].
- [4] R. Barate *et al.* [LEP Working Group for Higgs boson searches and ALEPH Collaboration], Phys. Lett. B **565** (2003) 61 [arXiv:hep-ex/0306033].
- [5] [CDF Collaboration and D0 Collaboration], arXiv:0911.3930 [hep-ex]; arXiv:0903.4001 [hep-ex].
- [6] LEP Electroweak working group, <http://www.cern.ch/LEPEWWG/> .
- [7] S. L. Glashow, J. Iliopoulos and L. Maiani, Phys. Rev. D **2** (1970) 1285.
- [8] H. Arason, D. J. Castano, B. Keszthelyi, S. Mikaelian, E. J. Piard, P. Ramond and B. D. Wright, Phys. Rev. D **46** (1992) 3945.
- [9] H. E. Haber, G. L. Kane and T. Sterling, Nucl. Phys. B **161** (1979) 493; J. F. Gunion, R. Vega and J. Wudka, Phys. Rev. D **42** (1990) 1673; P. Bamert and Z. Kunszt, Phys. Lett. B **306** (1993) 335 [arXiv:hep-ph/9303239]; A. G. Akeroyd, Phys. Lett. B **368** (1996) 89 [arXiv:hep-ph/9511347]; A. Barroso, L. Brucher and R. Santos, Phys. Rev. D **60** (1999) 035005 [arXiv:hep-ph/9901293]; L. Brucher and R. Santos, Eur. Phys. J. C **12** (2000) 87 [arXiv:hep-ph/9907434].
- [10] D. R. T. Jones and S. T. Petcov, Phys. Lett. B **84** (1979) 440; R. N. Cahn and S. Dawson, Phys. Lett. B **136** (1984) 196 [Erratum-ibid. B **138** (1984) 464]; D. A. Dicus and S. S. D. Willenbrock, Phys. Rev. D **32** (1985) 1642; K. i. Hikasa, Phys. Lett. B **164** (1985) 385 [Erratum-ibid. **195B** (1987) 623]; G. Altarelli, B. Mele and F. Pitolli, Nucl. Phys. B **287** (1987) 205. W. Kilian, M. Kramer and P. M. Zerwas, Phys. Lett. B **373** (1996) 135 [arXiv:hep-ph/9512355].
- [11] T. Han, G. Valencia and S. Willenbrock, Phys. Rev. Lett. **69** (1992) 3274 [arXiv:hep-ph/9206246]; T. Figy, C. Oleari and D. Zeppenfeld, Phys. Rev. D **68**, 073005

- (2003) [arXiv:hep-ph/0306109]; P. Nason and C. Oleari, JHEP **1002** (2010) 037; M. Ciccolini, A. Denner and S. Dittmaier, Phys. Rev. D **77** (2008) 013002 [arXiv:0710.4749 [hep-ph]].
- [12] P. Bolzoni, F. Maltoni, S. O. Moch and M. Zaro, Phys. Rev. Lett. **105**, 011801 (2010), arXiv:1003.4451 [hep-ph].
- [13] H. M. Georgi, S. L. Glashow, M. E. Machacek and D. V. Nanopoulos, Phys. Rev. Lett. **40** (1978) 692 .
- [14] D. Graudenz, M. Spira and P. M. Zerwas, Phys. Rev. Lett. **70** (1993) 1372; M. Kramer, E. Laenen and M. Spira, Nucl. Phys. B **511** (1998) 523 [arXiv:hep-ph/9611272]; R. V. Harlander and W. B. Kilgore, Phys. Rev. Lett. **88** (2002) 201801 [arXiv:hep-ph/0201206]; C. Anastasiou and K. Melnikov, Nucl. Phys. B **646** (2002) 220 [arXiv:hep-ph/0207004]; S. Catani, D. de Florian, M. Grazzini and P. Nason, JHEP **0307** (2003) 028 [arXiv:hep-ph/0306211]; U. Aglietti, R. Bonciani, G. Degrossi and A. Vicini, Phys. Lett. B **595** (2004) 432 [arXiv:hep-ph/0404071]; G. Degrossi and F. Maltoni, Phys. Lett. B **600** (2004) 255 [arXiv:hep-ph/0407249].
- [15] A. Heister *et al.* [ALEPH Collaboration], Phys. Lett. B **544** (2002) 16; P. Abreu *et al.* [DELPHI Collaboration], Phys. Lett. B **507** (2001) 89 [arXiv:hep-ex/0104025]; P. Achard *et al.* [L3 Collaboration], Phys. Lett. B **534** (2002) 28 [arXiv:hep-ex/0203016]; Phys. Lett. B **568**, (2003) 191 [arXiv:hep-ex/0307010]; G. Abbiendi *et al.* [OPAL Collaboration], Phys. Lett. B **544** (2002) 44 [arXiv:hep-ex/0207027].
- [16] B. Abbott *et al.* [D0 Collaboration], Phys. Rev. Lett. **82** (1999) 2244 [arXiv:hep-ex/9811029]; V. M. Abazov *et al.* [D0 Collaboration], Phys. Rev. Lett. **101** (2008) 051801 [arXiv:0803.1514 [hep-ex]]; Phys. Rev. Lett. **102**, 231801 (2009) [arXiv:0901.1887 [hep-ex]].
- [17] A. A. Affolder *et al.* [CDF Collaboration], Phys. Rev. D **64** (2001) 092002 [arXiv:hep-ex/0105066]; T. Aaltonen *et al.* [CDF Collaboration], Phys. Rev. Lett. **103** (2009) 061803 [arXiv:0905.0413 [hep-ex]].
- [18] D. Y. Bardin and G. Passarino, “The standard model in the making: Precision study of the electroweak interactions”, *Clarendon Press, Oxford (1999) 685 p.*
- [19] T. Appelquist and M. S. Chanowitz, Phys. Rev. Lett. **59**, 2405 (1987) [Erratum-ibid. **60** (1988) 1589].

- [20] D. A. Dicus and H. J. He, Phys. Rev. D **71** (2005) 093009 [arXiv:hep-ph/0409131].
- [21] V. A. Miransky, M. Tanabashi and K. Yamawaki, Phys. Lett. B **221**, 177 (1989); Mod. Phys. Lett. A **4** (1989) 1043.
- [22] D. Anselmi, Eur. Phys. J. C **65**, 523 (2010) [arXiv:0904.1849 [hep-ph]].
- [23] M. Antola, M. Heikinheimo, F. Sannino and K. Tuominen, JHEP **1003**, 050 (2010) [arXiv:0910.3681 [hep-ph]].
- [24] C. T. Hill, Phys. Lett. B **345**, 483 (1995) [arXiv:hep-ph/9411426]; C. T. Hill and E. H. Simmons, Phys. Rept. **381**, 235 (2003) [Erratum-ibid. **390**, 553 (2004)] [arXiv:hep-ph/0203079].
- [25] M. E. Peskin and T. Takeuchi, Phys. Rev. Lett. **65**, 964 (1990); Phys. Rev. D **46**, 381 (1992).
- [26] J. Fleischer, O. V. Tarasov and F. Jegerlehner, Phys. Lett. B **319**, 249 (1993).
- [27] L. Resnick, M. K. Sundaresan and P. J. S. Watson, Phys. Rev. D **8** (1973) 172.
- [28] E. Braaten and J. P. Leveille, Phys. Rev. D **22** (1980) 715; N. Sakai, Phys. Rev. D **22** (1980) 2220; T. Inami and T. Kubota, Nucl. Phys. B **179** (1981) 171; S. G. Gorishnii, A. L. Kataev and S. A. Larin, Sov. J. Nucl. Phys. **40** (1984) 329 [Yad. Fiz. **40** (1984) 517].
- [29] J. R. Ellis, M. K. Gaillard and D. V. Nanopoulos, Nucl. Phys. B **106** (1976) 292.
- [30] B. W. Lee, C. Quigg and H. B. Thacker, Phys. Rev. D **16** (1977) 1519; G. Pocsik and T. Torma, Z. Phys. C **6** (1980) 1; T. G. Rizzo, Phys. Rev. D **22** (1980) 722; W. Y. Keung and W. J. Marciano, Phys. Rev. D **30** (1984) 248.
- [31] M. A. Shifman, A. I. Vainshtein, M. B. Voloshin and V. I. Zakharov, Sov. J. Nucl. Phys. **30** (1979) 711 [Yad. Fiz. **30** (1979) 1368].
- [32] R. N. Cahn, M. S. Chanowitz and N. Fleishon, Phys. Lett. B **82** (1979) 113; L. Bergstrom and G. Hulth, Nucl. Phys. B **259** (1985) 137 [Erratum-ibid. B **276** (1986) 744].
- [33] J. R. Ellis, M. K. Gaillard, D. V. Nanopoulos and C. T. Sachrajda, Phys. Lett. B **83** (1979) 339. T. G. Rizzo, Phys. Rev. D **22** (1980) 178 [Addendum-ibid. D **22** (1980) 1824].
- [34] A. Grau, G. Panchieri and R. J. N. Phillips, Phys. Lett. B **251** (1990) 293.
- [35] S. Mrenna and J. D. Wells, Phys. Rev. D **63** (2000) 015006 [arXiv:hep-ph/0001226].

- [36] F. Maltoni, <http://maltoni.home.cern.ch/maltoni/TeV4LHC/SM.html> .
- [37] M. Grazzini, <http://theory.fi.infn.it/grazzini/hcalculators.html>; D. de Florian and M. Grazzini, Phys. Lett. B **674**, 291 (2009) [arXiv:0901.2427 [hep-ph]].
- [38] J. M. Butterworth, A. R. Davison, M. Rubin and G. P. Salam, Phys. Rev. Lett. **100**, 242001 (2008) [arXiv:0802.2470 [hep-ph]].
- [39] J. A. Aguilar-Saavedra *et al.* [ECFA/DESY LC Physics Working Group], arXiv:hep-ph/0106315, http://tesla.desy.de/new_pages/TDR_CD/start.html .
- [40] C. Amsler *et al.* [Particle Data Group], Phys. Lett. B **667** (2008) 1.